The DOI for this manuscript is doi: 10.1175/BAMS-D-16-0256.1

The Dynamics-Aerosol-Chemistry-Cloud Interactions in West Africa field campaign:

Overview and research highlights

C. Flamant[1], P. Knippertz[2], A. H. Fink[2], A. Akpo[3], B. Brooks[4,5], C. J. Chiu[6], H. Coe[7], S. Danuor[8], M. Evans[4,9], O. Jegede[10], N. Kalthoff[2], A. Konaré[11], C. Liousse[12], F. Lohou[12], C. Mari[12], H. Schlager[13], A. Schwarzenboeck[14], B. Adler[2], L. Amekudzi[8], J. Aryee[8], M. Ayoola[10], A. M. Batenburg[15], G. Bessardon[5], S. Borrmann[15], J. Brito[14], K. Bower[7], F. Burnet[16], V. Catoire[17], A. Colomb[14], C. Denjean[16], K. Fosu-Amankwah[8], P. G. Hill[6], J. Lee[9], M. Lothon[12], M. Maranan[2], J. Marsham[4,5], R. Meynadier[1], J.-B. Ngamini[18], P. Rosenberg[5], D. Sauer[13], V. Smith[4], G. Stratmann[13], J. W. Taylor[7], C. Voigt[13,19], V. Yoboué[11]

[1]Laboratoire Atmosphères Milieux Observations Spatiales, Sorbonne Universités, UPMC Université Paris 06, UVSQ and CNRS, Paris, France

[2]Institute of Meteorology and Climate Research, Karlsruhe Institute of Technology, Karlsruhe, Germany

[3]Laboratoire de Physique du Rayonnement, Université Abomey-Calavi, Cotonou, Benin

[4]National Centre for Atmospheric Science

[5]University of Leeds, Leeds, United Kingdom

[6]Department of Meteorology, the University of Reading, Reading, United Kingdom

[7]School of Earth and Environmental Sciences, University of Manchester, Manchester, United Kingdom

[8]Department of Physics, Kwame Nkrumah University of Science and Technology, Kumasi, Ghana

[9]Wolfson Atmospheric Chemistry Laboratories/National Centre for Atmospheric Science, University of York, York, United Kingdom

[10]Department of Physics and Engineering Physics, Obafemi Awolowo University, Ile-Ife, Nigeria

[11]Laboratoire de Physique de l'Atmosphère et de Mécanique des Fluides, Université of Cocody, Abidjan, Ivory Coast

[12]Laboratoire d'Aérologie, Université de Toulouse and CNRS, Toulouse, France

[13]Institut für Physik der Atmosphäre, Deutsches Zentrum für Luft- und Raumfahrt, Oberpfaffenhofen Wessling, Germany

[14]Laboratoire de Météorologie Physique, Université Blaise Pascal, CNRS, Clermont-Ferrand, France

[15]Max Planck Institute for Chemistry/Johannes Gutenberg University Mainz, Mainz, Germany

[16]Centre National de Recherches Météorologiques, Météo-France and CNRS, Toulouse, France

[17]Laboratoire de Physique et Chimie de l'Environnement et de l'Espace, Université d'Orléans and CNRS, Orléans, France

[18]Agence pour la sécurité de la navigation aérienne en Afrique et à Madagascar, Dakar, Senegal

[19]Institut für Physik der Atmosphäre, University Mainz, Mainz, Germany

Corresponding Author: Cyrille Flamant (cyrille.flamant@latmos.ipsl.fr)

Corresponding author address: LATMOS, Université Pierre et Marie Curie, Boîte 102, 4 place Jussieu, 75252 Paris cedex 05, FRANCE

Abstract

The EU-funded project DACCIWA (Dynamics-Aerosol-Chemistry-Cloud Interactions in West Africa) investigates the relationship between weather, climate, and air pollution in southern West Africa, an area with rapid population growth, urbanisation, and increase in anthropogenic aerosol emissions. The air over this region contains a unique mixture of natural and anthropogenic gases, liquid droplets and particles, emitted in an environment, in which multi-layer clouds frequently form. These exert a large influence on the local weather and climate, mainly due to their impact on radiation, the surface energy balance, and thus the diurnal cycle of the atmospheric boundary layer.

In June and July 2016, DACCIWA organized a major international field campaign in Ivory Coast, Ghana, Togo, Benin, and Nigeria. Three supersites in Kumasi, Savè, and Ile-Ife conducted permanent measurements and 15 Intensive observation periods. Three European aircraft together flew 50 research flights between 27 June and 16 July 2016 for a total of 155 hours. DACCIWA scientists launched weather balloons several times a day across the region (772 in total), measured urban emissions, and evaluated health data. The main objective was to build robust statistics of atmospheric composition, dynamics, and low-level cloud properties in various chemical landscapes to investigate their mutual interactions.

This article presents an overview of the DACCIWA field campaign activities as well as some first research highlights. The rich data obtained during the campaign will be made available to the scientific community and help to advance scientific understanding, modeling, and monitoring the atmosphere over southern West Africa.

78

79 **Capsule Summary**:

80

81 Unprecedented ground-based and aircraft measurements in June-July 2016 in
82 southern West Africa characterize atmospheric composition and dynamics, low-level
83 cloud properties, the diurnal cycle, and air pollution impacts on health.

1. Introduction

Tropical Africa is a region with particularly poor operational monitoring of the atmosphere and its constituents. Moreover, the observational network has degraded in recent decades with many measurements being made using analogue instruments failing to provide high-quality, highly-resolved observations to the weather services and the research community. Advanced ground-based vertical profiling in situ and remote sensing systems, which have been installed in developed countries in recent decades, are – with very few exceptions – absent in tropical Africa. In addition, weather forecasting and climate models are known to have particular deficiencies in this region. For example, climate projections of rainfall in West Africa, as reviewed in the last Intergovernmental Panel on Climate Change assessment report (IPCC 2013), have not improved over the penultimate report. Finally, weather forecasts of convective rainfall have a particularly poor skill in the West African region (e.g., Fink et al. 2011).

So far, very few field experiments have been conducted in sub-Saharan Africa, the largest of which were the GARP Atlantic Tropical Experiment (GATE; Kuettner, 1974) and the African Monsoon Multidisciplinary Analysis (AMMA; Redelsperger et al. 2006, Lebel et al. 2010). The preparation and execution of such international field campaigns has proved to be extremely challenging. Yet, thanks to their rich and widely accessible databases, GATE and AMMA have advanced our understanding of the West African climate systems. In this article, the measurements made during the most recent large international field campaign in Africa, DACCIWA (Dynamics-aerosol-chemistry-cloud interactions in West Africa, http://www.dacciwa.eu, Knippertz et al. 2015a), are described along with preliminary research highlights.

The EU-funded DACCIWA 2016 field campaign took place in southern West Africa (SWA) in June-July 2016, one year later than initially planned due to the Ebola epidemic, and involved upper-air, ground, and aircraft measurements in five West African countries. While AMMA focussed on the Sahel and GATE on the eastern tropical Atlantic, DACCIWA targets the very densely populated and chemically diverse Guinea coastal region, which is currently undergoing rapid socio-economic changes. An explosively growing population, massive urbanisation, unregulated deforestation, and increasing anthropogenic emissions modify the composition of the atmosphere. Emissions from charcoal fires, traffic, and burning rubbish as well as power plants, ship traffic, oil rigs, and tropical forest influence atmospheric composition over SWA. In addition, monsoon winds bring sea salt and other oceanic compounds from the south, while large biomass burning (BB) plumes are advected from the southern hemisphere, and northerly winds bring dust from the Sahel and Sahara, making the air over the coastal region of West Africa a unique mixture of various gases, liquid and solid particles. The atmospheric composition (gases and particles), the influence of anthropogenic pollutants and their secondary chemistry as well as impacts on humans and ecosystems have never been studied in detail over this region.

At the same time, this region is characterized by a complex meteorology. Multi-layer cloud decks frequently form in this environment and exert a large influence on the local weather and climate, mainly due to their impact on radiation, the surface energy balance, and thus the diurnal cycle of the atmospheric boundary layer, which in turn is connected to the triggering of convection. In particular, the mechanisms involved in the formation and dissolution of clouds with bases below 300

m above ground level (AGL, e.g., Schuster et al. 2013) and mid-level clouds (Stein et al. 2011; Gonou et al. 2012) are not well understood to date, mostly because of a lack of adequate in-situ and remote-sensing observations. Furthermore, climate models are known to misrepresent low and mid-level cloudiness in SWA, where the frequency and amount of such clouds is substantial, especially during late night and early morning hours (van der Linden et al. 2015; Hannak et al. 2017). The supposed cooling effect of mid-level clouds is currently missing in global climate models (Bourgeois et al., 2016). Such errors and the lack of appropriate compositional observations hinder advancing knowledge of chemistry-aerosol-cloud interactions in such a complex chemical environment (Knippertz et al. 2015b).

A review of the meteorological and chemical measurements made during the field campaign (see **Table 1** for the timeline of the DACCIWA experiment) and some preliminary results are presented in this paper with the aim to make researchers aware of a new rich experimental data set for SWA. We expect that DACCIWA data will widely be used by researchers around the world in the next two decades. The meteorological and chemical conditions during the campaign are presented in Knippertz et al. (2017, submitted). As part of this campaign, three research aircraft based in Togo flew targeted coordinated missions over SWA (**Figure 1**). Section 2 presents the aircraft capabilities and the flight objectives. In addition to the flights, DACCIWA scientists set up three highly instrumented measuring sites inland in Ghana, Benin, and Nigeria. The instruments deployed on the ground and the experimental strategies are detailed in Section 3. A coordinated effort to launch weather balloons several times a day across the region was also conducted. The network of operational stations and stations specifically set-up at DACCIWA sites are described in Section 4. Urban emissions were measured in Abidjan and Cotonou, and health

data evaluated in Abidjan, which are reported in Section 5. The field campaign was supported by a satellite component which is described in Section 6. Finally, selected campaign highlights are presented in an integrative framework in Section 7 and conclusions are given in Section 8.

2. Aircraft Campaign

The main objective for the aircraft detachment was to build robust statistics of cloud properties in SWA in different chemical landscapes: from the background state over the Gulf of Guinea (marine aerosols or mix between marine aerosols and BB aerosols from the Southern Hemisphere) to ship/flaring emissions to the coastal strip of polluted multi-million-inhabitant cities to the agricultural areas and forest areas further north, and eventually dust from the Sahel/Sahara. An ancillary objective of the detachment was to contribute to the reduction of uncertainties on emissions from big cities, ship and oil rigs, as well as biogenic emissions from vegetation. Flight activities were coordinated with the ground-based (Section 3) and urban components (Section 5).

The project brought together three research aircraft from three countries: the German Deutsches Zentrum für Luft- und Raumfahrt (DLR) Falcon 20, the French Service des Avions Français Instrumentés pour la Recherche en Environnement (SAFIRE) ATR 42 and the British Antarctic Survey (BAS) Twin Otter (**Figure S1**). Scientific flights took place between 29 June and 16 July 2016 (**Table 1**). The entire aircraft detachment fell into the so-called post-onset period (see Knippertz et al., 2017, submitted), with a well-established monsoon and thus relatively dry conditions along the Gulf of Guinea coast with frequent formation of low clouds. The three research

aircraft were deployed from the Lomé Military Airport (Togo) and conducted a total of over 155 science flight hours (**Table 2**), including hours sponsored through three European Facility for Airborne Research (EUFAR) projects (see **Table 2**). The aircraft were used in different ways based on their strengths, but all three had comparable instrumentation with the capability to measure general meteorology, gas-phase chemistry, aerosols, and clouds, thereby generating a rich dataset of atmospheric conditions across the region (see **Table S1** for detailed payloads for each aircraft).

Flights were coordinated from the DACCIWA Operations Center (DOC, www.dacciwa.sedoo.fr) located in Lomé. The DOC began operations on 25 June to prepare forecasts for the first potential flight operations and to test communications with the ground-based supersites in Savè (Benin), Kumasi (Ghana), and Ile-Ife (Nigeria). Throughout the campaign, the aircraft flights were monitored live from the DOC, in liaison with the ground-based facilities. Two daily briefing meetings were organized at the DOC during the period of the aircraft detachment, at 1100 and 1900 UTC between 25 June and 15 July, which included overviews of the meteorology and chemistry/aerosol conditions prepared by the forecast team (composed of DACCIWA scientists and agents from the Direction Générale de la Météorologie Nationale Togo).

Eight types of flight objectives were conducted over Togo and neighboring countries Ivory Coast, Ghana, and Benin, see **Fig. 1**):

1. Low-level clouds (LLCs): Describe the atmospheric dynamics, thermodynamics, radiation, composition, and LLCs properties inland along the monsoon flow and document the diurnal cycle of all these variables, as they evolved through stratus to stratocumulus to cumulus or cumulus congestus. Based on

the stratus cloud climatology reported in van der Linden et al. (2015), two preferred regions of operations were selected: (i) over southern Ghana and Ivory Coast, where satellite observations show the highest occurrence frequency, and (ii) over Benin, where stratus clouds are observed often as well, but not as extensively as those over Ivory Coast. The flights were organized along three axes: (i) Lomé-Savè, (ii) Lomé-Accra-Kumasi, and (iii) Lomé-Abidjan (see **Fig. 1** and **Table S3**). The former two flights allowed liaising aircraft measurements with observations at the Savè and Kumasi supersites. Stratus cloud properties were sampled both within and outside of the pollution plumes of major cities.

2. Land-sea breeze clouds: Document the impact of land-sea breeze clouds on the scavenging and ventilation of pollutants (chemical compounds and aerosols) along the monsoon flow, downstream of the urbanized coastal strip.
3. Biogenic emission: Document biogenic gaseous and aerosol emissions across and along the south–north climatological gradient of vegetation in SWA (including primary forests) and downstream of major polluted cities to study the interaction of biogenic and anthropogenic aerosols (see **Table S3**).
4. City emissions: Document the atmospheric dynamics, thermodynamics, radiation, and composition upstream and downstream of polluted coastal cities (both budget and ageing type analyses) (see **Table S3**). For the sake of robust statistics, only a few big cities (Accra, Kumasi, Lomé, Cotonou and Abidjan) were targeted. Coordination with the urban emission campaign in Abidjan (see Section 5) was achieved.
5. Dust and BB aerosols: Document the plumes from fires in the southern hemisphere and dust aerosol from Saharan/Sahelian sources transported to

SWA and likely impacting the air quality in and around cities and the life cycle of stratus (through direct radiative or indirect effects) (see **Table S3**).

6. APSOWA (Air Pollution from Shipping and Oil platforms of West Africa, funded by EUFAR): Characterize the gaseous and particulate pollutants emitted by shipping and oil/gas extraction platforms (Jubilee oil field off-shore of Ghana and Espoir, Panther and Lion oil fields offshore of Ivory Coast, see **Fig. 1** and **Table S3**).
7. MICWA (MId-level Clouds over West Africa, funded by EUFAR): Document dynamic/thermodynamic genesis and lysis processes of mid-level cloud decks in order to understand the respective roles of radiative, turbulence, and synoptic-scale subsidence processes.
8. OLACTA (Observing the Low-level Atmospheric Circulation in the Tropical Atlantic, funded by EUFAR): Document low-level atmospheric circulation over the Gulf of Guinea, which develops in response to an equatorial upwelling, and has a significant impact on air-sea interactions, moisture transport, cloud development, and pollution ventilation in the coastal areas of SWA (Leduc-Leballeur et al. 2013).

Flight plans were engineered such that they could accommodate several objectives (e.g., stratus and land-sea breeze clouds and urban/biogenic emissions). Times, locations, and scientific objectives of all flights conducted during the campaign are given in **Table S2**. Instruments calibration and inter-comparison exercises were also conducted to identify problems and assess differences between similar instruments embarked on the different aircraft, using specifically designed protocols for (i) aerosols and clouds, (ii) chemistry, and (iii) radiation.

3. Ground-based Campaign

LLCs are of primary importance for the regional weather, climate, and air quality due to radiative effects, impacts on the convective boundary layer (CBL) development, and interactions with pollutants. The ground-based campaign was conducted in areas strongly affected by LLCs. Measurements were designed to identify the controlling processes and factors for LLC formation and to investigate LLC effects on CBL conditions.

Intensive measurements were performed from 14 June to 30 July 2016 (**Table 1**) at three supersites forming a west–east transect along the Guinean coast: Kumasi (Ghana), Savè (Benin), Ile-Ife (Nigeria) (**Fig. 1**):

1. The Kumasi site (6°40'48.56''N, 1°33'37.76''E, 266 m above sea mean level level, AMSL) on the estates of KNUST (Kwame Nkrumah University of Science and Technology) was operated by NCAS (National Centre for Atmospheric Science) with assistance from KNUST;
2. The site at Savè (8°00'03.6"N, 2°25'41.1"E, 166 m AMSL) was jointly operated by KIT (Karlsruhe Institute of Technology) and UPS (Université Toulouse III - Paul Sabatier, Laboratoire d'Aérologie), and hosted by INRAB (Institut National de Recherche Agronomique du Benin). Some instruments were deployed at the Savè airfield (8°01'04.4"N, 2°27'50.8"E, 180 m AMSL), located 4 km east of the INRAB site;
3. The Ile-Ife site (7°33'11.52"N, 4°33'26.70"E, 274 m AMSL) was on the campus of Obafemi Awolowo University (OAU), at the same location as the permanent meteorological station, OAU-Met.

A comprehensive set of instruments was deployed at the three sites (**Table S4**). Capacity building efforts were undertaken at the Savè and Kumasi supersites, involving operational and academic research partners, as well as students when possible. Surface stations measuring the mean meteorological parameters, surface radiation and energy balance components, and soil temperature and humidity provided the lower boundary conditions and, at the same time, the LLCs impact on the radiation balance at the surface. Thermodynamics and dynamics in the lower atmosphere were monitored continuously by active (wind profilers, Doppler lidars, sodars) and passive (microwave radiometers) remote sensing systems. In addition to radiosondes launched at synoptic times, tethered radiosondes in Ile-Ife and frequent radiosondes in Kumasi and Savè were launched in regular intervals during Intensive Operation Periods (IOPs). These measurements focus on the detection of the nocturnal low level jet (LLJ), monsoon and Harmattan flows, African Easterly Jet (AEJ), and the tropospheric stratification. Cloud characteristics such as cloud base, top, and cover as well as the spatial and temporal evolution of precipitation and cloud drop-size distribution were monitored by a set of in-situ and remote sensing devices (distrometers, rain gauges, cloud radar, rain radar, infrared radiometer, cloud camera). Chemistry and aerosol measurements complete this data set. Finally, two Remotely Piloted Aircraft Systems (RPASs), Aladina and OVLI, were operated in Savè during the aircraft campaign by Innovationsgesellschaft Technische Universität Braunschweig. All measured parameters are listed in **Table S4**. The applied measurement strategy, e.g., scan patterns and radiosounding frequency, was optimised to capture various atmospheric processes expected from high-resolution simulations performed in preparation of the campaign. These include horizontal advection from the Guinea coast and triggering of new clouds upstream of existing clouds due to an upward shift of the LLJ in cloudy areas (Adler et al. 2017).

317

318 The ground-based campaign started two weeks before, and continued for two
319 weeks after the aircraft campaign. During this period, all systems were operated
320 continuously, except of the radiosondes and the RPASs. In Kumasi and Savè,
321 radiosondes were launched every morning at 0600 UTC. This time was selected
322 because the LLC cover was expected to be largest. In total, fifteen IOPs were
323 conducted at all three sites, seven of which during the aircraft campaign (see **Table**
324 **1**), running for 24 hours from 1800 UTC. During an IOP, 4 radiosondes were launched
325 every 6 hours and frequent or tethered radiosoundings were performed in between,
326 every 1 to 3 hours depending on the supersite. In Savè, RPAS Ovli flew vertical profiles
327 in the afternoon during periods when no frequent radiosoundings were launched.
328 RPAS Aladina, equipped with a turbulence probe, performed flight patterns
329 consisting of vertical profiles and horizontal legs during periods when LLCs were
330 present in the morning, when the LLCs were breaking up, and in the evening during
331 the transition phase towards stable conditions.

332

333 During the 7 weeks of measurements, LLCs were observed almost every night at the
334 three sites. However, strong variations in the spatio-temporal characteristics of LLCs
335 and LLJs occurred not only between the different supersites, but also from day to
336 day at the individual sites. The cloud base height varied from near the ground to
337 several hundred meters AGL, and the vertical extent ranged from several hundred to
338 more than a thousand meters. LLC formation occurred between 2000 and 0600 UTC.
339 LLCs normally started to lift simultaneously with the growth of the CBL and broke up
340 progressively in the early afternoon. This strong variability is supposed to be
341 associated with, e.g., the nocturnal LLJ strength and depth, the transition layer
342 between the monsoon flow and Harmattan, the atmospheric stratification, and the

343 position of the AEJ and the existence of mid- and upper level clouds. These
344 parameters change on day-to-day to monthly scales.
345
346 **4. Radiosonde Campaign**
347
348 Operational upper-air stations are very sparsely distributed over West Africa, resulting
349 in a need to enhance upper-air observations during the DACCIWA experimental
350 period. Building on the experience during AMMA (cf., Parker et al. 2008), existing
351 infrastructure and personal connections, the upper air network was successfully
352 augmented during June-July 2016 to a spatial density unprecedented for SWA. From
353 its outset, the DACCIWA radiosonde campaign had three pillars (a) enhancing
354 soundings at operational or quiescent AMMA radiosonde stations; (b) launching
355 sondes at DACCIWA supersites and two additional DACCIWA field sites; and (c)
356 collecting standard and – if possible – high-resolution data from other operational
357 radiosounding stations.
358
359 During the pre-campaign investigation of the status of operational stations, three
360 surprises were encountered. Firstly, the Vaisälä ground station furnished in 2006 by
361 AMMA to the NIMET (Nigerian Meteorological Agency) station of Abuja (see **Table 3**
362 for WMO number) was in operational use; Abuja regularly conducted 1200 UTC
363 soundings, but hardly any of them were received on the Global Telecommunication
364 System (GTS) due to transmission problems. Secondly, Cotonou (Benin) resumed 1200
365 UTC soundings in September 2012 using the MODEM ground station provided by
366 AMMA. However, while being on the GTS, the use of TEMPS from Cotonou in
367 databases and weather prediction appeared to be impeded by missing meta-
368 information. Thirdly, NIMET operated four additional radiosonde stations at Lagos,

Kano, Enugu, and Calabar (see **Figure S2** for station locations), from which only Kano TEMPs sporadically appeared on the GTS before the campaign.

The management of soundings at Abidjan, Cotonou, and Parakou was subcontracted to a private company with a success rate of almost 100% (**Figure S3**). The existing collaboration with the Ghana Meteorological Agency (GMET) enabled us to conduct experimental soundings at their headquarters in Accra. In cooperation with the Lamto Geophysical Observatory and the Université Félix Houphouët-Boigny, radiosondes were launched at Lamto, some 150 km inland of Abidjan. As a consequence, three coastal and three near-coastal stations were active (Figure S3), resulting in an unprecedented sampling of the strength and depth of the low-level monsoon inflow and the land-sea breeze. Capacity building efforts were undertaken at Lamto and Accra, where operations were mainly executed by a team of German and African students, with invaluable help of GMET and Lamto staff. Both stations made up to five soundings per day, with the additional 0900 UTC soundings occurring at the diurnal peak of cloudiness associated with low-level stratus (van der Linden et al. 2015). Finally, 0600 UTC soundings were performed systematically in Kumasi and Savè as explained in Section 3. Launching statistics and radiosonde types can be inferred from **Figs S2** and **S3**, and **Table 4**. Altogether some 772 radiosondes were launched. In addition, TEMP and, if possible, high-resolution 1200 UTC sounding data for June-July 2016 were acquired for Nigerian operational stations indicated in yellow in **Figs S2** and **S3**. Thanks to an excellent collaboration with the German Weather Service, e-mail real-time transmissions of FM 35 TEMP Mobile messages to the GTS were made for Lamto, Kumasi, Accra, and Parakou. The subcontracted company and ASECNA (Agence pour la Sécurité de la Navigation Aérienne en Afrique et à Madagascar) ensured real-time transmission of Cotonou

and Abidjan whereas FM 94 BUFFR TEMP mobile messages from Savè were e-mailed to and ingested by Météo France numerical weather prediction models.

The high-resolution data will contribute significantly to assessing and monitoring the time evolution of wind-stability-humidity regimes that are related to certain types of convection. **Figure 3** shows a time-height diagram of zonal wind speed and barbs for Parakou. A thunderstorm in the afternoon of 8 July 2016 was associated with high values of low-level shear between monsoonal southwesterlies and mid-level easterlies, whereas the non-thundery rainfall between 11 and 14 July 2016 occurred in a strong and relatively deep low-level westerly regime with low shear. It is reminiscent of monsoon or vortex rainfall as discussed in Fink et al. (2006).

5. Urban Campaign

The urban campaign was conducted on four sites representative of the main combustion sources specific to SWA (traffic, domestic fire, and waste burning), three of which are located in Abidjan (Ivory Coast) and one in Cotonou (Benin) (**Fig. 1**). The urban campaign took place on 4–10 July (Abidjan) and 10–13 July 2016 (Cotonou). The instrumented four sites are:

1. Yopougon (Abidjan): within a courtyard surrounded by houses using domestic fires for cooking, where more than twenty women use woodfires for fish smoking;
2. Adjamé (Abidjan): on the roof of a pharmacy, above a large street with frequent traffic jams and close to a large crossroad;
3. Akouedo (Abidjan): on the roof of a building built on the biggest waste burning hill of the country in activity since 1965;

4. Dantokpa (Cotonou): in front of the biggest market of Benin, on the balcony of a building near a crossing with a high traffic density. This site is impacted by emissions from both four- and two- wheels using gasoline fuel, as opposed to Abidjan where mainly diesel four-wheel vehicles are in use.

These measurements are combined with modeling and satellite data, aiming to link emission sources, air pollution, and health impacts in terms of lung inflammation and diseases in SWA. The July 2016 urban campaign is part of a long-term effort initiated in December 2014, which will continue until March 2017. The aim of the of long-term campaign is to calculate in situ dose-response functions for each studied sources on these four sites based on air pollution datasets and epidemiological surveys. The details of the measurements strategy are given in **Table S5**.

The specific aims of short-term July 2016 urban campaign are:

1. to calculate in-situ dose-inflammatory response ratios for each studied sources on the four sites. Doses in the respiratory tracts are obtained from atmospheric concentrations using a model. Air pollution experiments include three impactors running in parallel three times in each campaign in the same conditions, in order to determine aerosol chemical composition and their pro-oxidant capacity by size, as well as in vitro inflammatory biomarkers to derive inflammatory response. As an example for July 2016, **Figure 4** shows the carbonaceous aerosol importance in the aerosol mass by size, with higher ratios in Abidjan than in Cotonou. The highest mass concentration is found for the domestic fire site;
2. to establish spatial distributions of gaseous components (e.g., NO_2, O_3) in Abidjan and Cotonou with multi-site deployment of passive samplers;

3. to measure emission factors for gases and particles for the main African specific urban sources (domestic fires with different woods and charcoal, charcoal making, and many representative two- and four-wheels vehicles) in the streets but also in combustion chambers. This will lead to a revised emission inventory;
4. to assess personal exposures to $PM_{2.5}$ and aerosol chemistry emitted from domestic fire emissions for housewifes, waste burning emissions for students and motor vehicle emissions for drivers. Participants were equipped with personal impactors and followed three consecutive days (night and day).

6. Satellite

Observing aerosols, clouds, and precipitation from space over the SWA region remains challenging. The prevailing clouds make it difficult to properly monitor aerosols due to a lack of clear-sky conditions required for aerosol retrieval. For clouds, Hill et al. (2016) found large differences between satellite cloud products particularly in high- and low-level cloud fractions. Different satellite rainfall retrieval approaches can also be associated with contrasting cloud sensitivities (e.g. Tompkins and Adebiyi (2012). Although active remote sensors like radar and lidar have better capability to probe cloud vertical structures, quantifying cloud properties is problematic because lidar backscatter is quickly attenuated with increasing cloud optical depth and radar signals are contaminated by ground clutter. Additionally, field campaigns dedicated to marine stratocumulus have shown evidence of an aerosol effect on warm rain suppression (van Zanten et al. 2005; Mann et al. 2014). While warm rain frequency may not be as high as convective precipitation frequency over SWA

(Mülmenstädt et al. 2015), the amount of warm rain and its susceptibility to aerosol perturbation have not been quantitatively determined over SWA.

Measurements from the DACCIWA field campaign have provided invaluable information for evaluating satellite retrievals, such as cloud products from the Spinning Enhanced Visible and InfraRed Imager (SEVIRI) aboard Meotosat, and a number of non-geostationary products, as shown in **Table 1**. We will evaluate satellite products in two ways. Firstly, direct comparisons of cloud and aerosol statistics can be made by collocating satellite overpasses with aircraft transects and the instrumented ground sites. Secondly, using these satellite-based cloud and aerosol properties as input to radiative transfer models, we will perform radiation closure studies, comparing the calculated irradiances against measurements. A total of eight flights were conducted for radiation closure studies (**Table S3**), including two dedicated calibration flights, which are necessary for correcting shortwave downwelling radiation measurements affected by the aircraft pitch and roll offsets and the offset of the radiometers relative to the aircraft. Combining the airborne radiation measurements with those from ground sites and the Geostationary Earth Radiation Budget (GERB) instrument aboard Meteosat, the campaign provides an excellent opportunity to close the radiation budget at the surface, the aircraft altitude, and the top of the atmosphere, which is crucial for evaluating not only column-integrated properties of clouds and aerosols, but also their vertical structures and boundaries in satellite products.

7. Campaign highlights

This section contains five examples of campaign observations. Whilst preliminary, they illustrate the enormously rich data resource obtained in June-July 2016 and its potential to solve some long-standing scientific questions in the area of interactions between atmospheric composition and meteorology over SWA. The first example illustrates how the three aircraft worked together and in liaison with the Savè supersite to characterize the diurnal cycle of low-level clouds over Benin. The second example illustrates the aircraft strategy designed to sample emission around and downstream of two big cities. The third example highlights how airborne radiation measurements will be used to investigate the quality of the space-borne radiative products. The fourth example demonstrates the value of having a network of well-instrumented supersites to simultaneously characterize the LLC evolution across SWA. The last example provides insights into the structure and composition of a massive BB plume, unexpectedly sampled by two of the aircraft during cloud-oriented missions.

a. Diurnal evolution of cloud-aerosol interactions on 5 July 2016

On 5 July 2016, the three aircraft SAFIRE ATR 42, DLR Falcon 20, and BAS Twin Otter flew on the same track from Lomé to Savè at different times of day (**Table S2**). As discussed by Knippertz et al. (2017), the period of aircraft operations was characterized by a high fraction of low clouds (over 85%).

The ATR 42 flew the Lomé-Savè track twice between 0800 and 1100 UTC (**Fig. 5g)**, the Falcon 20 twice between 1120 and 1500 UTC (**Fig. 5h)**, and the Twin Otter once between 1600 and 1750 UTC (**Fig. 5i**). This approach enabled investigation of the

524 stratus-to-cumulus diurnal cycle, as well as concurrent changes in aerosol properties.
525 All three aircraft were equipped with Passive Cavity Aerosol Spectrometer Probes
526 (PCASP, **Fig. 5a–c**) to measure aerosol concentration in the range 0.125–3 µm. Cloud
527 droplet number concentration (CDNC) profiles in **Fig. 5d–f** are from different types of
528 instruments: a Fast Cloud Droplet Probe (CDP) for the ATR 42, a CDP for the Twin
529 Otter and a Cloud and Aerosol Spectrometer (CAS) for the Falcon in the size range
530 of 3–50 µm (see **Table S1**). Data from the entire flights are shown in **Fig. 5a–f**.
531
532 Pollution was ubiquitous throughout the lower few kilometers of the atmosphere (**Fig.**
533 **5a–c**). In the morning, a two-layer structure was observed below 2 km AMSL with a
534 marked maximum in the developing CBL, below 500 m AMSL, and with evidence
535 that the aircraft passed through plumes of increased aerosol concentrations, likely
536 related to coastal cities upstream (**Fig. 5a**). During the ATR flight, large CDNC values
537 (in excess of 500 # cm^{-3}) were measured near the top of the CBL, indicative of the
538 polluted conditions affecting the clouds (**Fig. 5d**). Between 0800 and 0930 UTC, cloud
539 tops remained below 1 km and cloud cover was higher at the northern end of the
540 leg. In the vicinity of Savè, the stratocumulus base rose from 300 m to 500 m AGL
541 during the time of the ATR flight (**Figure 6**). Throughout the late morning and
542 afternoon, the low cloud deck became more broken and sparse (**Fig. 5e, f**), with
543 some developing into small cumuli with cloud tops growing to altitudes above 3 km
544 AMSL in the late afternoon (**Fig. 5f**). As observed in Savè, the cloud base reached
545 ~3000 m AGL (~3160 m AMSL) around 1700 UTC (**Fig. 6**). The high CDNC values
546 observed in the morning flight in the lowest kilometer of the atmosphere were
547 observed at higher altitudes in the late morning and afternoon. Aerosol
548 concentrations where observed to be mixed over greater depths than in the
549 morning, due to the development of the CBL (**Fig. 5b, c**). The large spread of aerosol

concentrations observed during the afternoon flights for a given altitude reflects the fact that the aircraft flew in and out of the urban plumes of Lomé and Cotonou.

Once fully validated and inter-compared, measurements made on this day with the three aircraft (and other "cloud-aerosol interaction" flights, **Table S3**) will be used to investigate the effects of the lower tropospheric dynamics / thermodynamics, as well as the direct and indirect effect of natural and anthropogenic aerosols, on the diurnal cycle of low cloud over different parts of SWA, and their representation in state-of-the-art models.

b. Urban emission mapping on 6 July 2016

On 6 July 2016, the three aircraft conducted coordinated flights across coastal SWA (**Table S2**) to sample the outflow from the cities of Abidjan, Accra, and the Takoradi thermal power plant (see **Fig. 7** for location). The ATR 42 was in the air between 0709 and 1502 UTC and refueled in Abidjan, while the Falcon 20 conducted one flight from 0941 to 1313 UTC. The end of the morning ATR flight, the beginning of the afternoon ATR flight, and the middle part of the Falcon flight were dedicated to exploring the Abidjan urban plume at various distances downstream of the city center, below 1 km AMSL. The Twin Otter flight took place between 1355 and 1637 UTC and was focused on Accra city emissions. During the post-onset period, strong pollution dispersion towards the northeast was observed from coastal cities as pointed out by Knippertz et al. (2017).

Figure 7a shows tracks from the three aircraft colored by altitude, NO_2 (indicative of high temperature combustion), carbon monoxide (CO, indicative of low

temperature combustion), and CH_4 (which has both an anthropogenic and a natural component). Low-level wind direction across the flight region was generally from a southwesterly direction. From all three aircraft, enhanced levels of the three pollutants can be seen immediately downwind of the sources, with the DLR Falcon 20 and SAFIRE ATR 42 also sampling the Abidjan and Accra plumes up to 80 km farther west. **Figure 7b** shows altitude vs. latitude cross sections of the outflow from Accra sampled by the BAS Twin Otter. Enhancements can be clearly seen for NO_2 (< 5 ppbv), CO (100 ppbv), and CH_4 (40 ppbv) and occur at different points along the transects, suggesting sources from different parts of the city (e.g., industrial vs. residential areas). The plots also show the vertical distribution of the plume, which – combined with an assessment of the boundary layer height and measurements made upwind of the city – will enable a calculation of the emission rate of NO_2, CO, and CH_4 from Accra.

The observations acquired on this and other "city emission" flights (**Table S3**) will be used to constrain emissions in dedicated atmospheric chemistry models and apportion the relative importance of the main anthropogenic emissions contributing to air quality degradation in and downstream of major coastal cities in SWA.

c. Dust outbreak and implications for radiation on 2 July 2016

On 2 July 2016, the ATR performed a calibration flight from 0940 to 1300 UTC that contained several transects from a rotating box pattern (see **Figure 8**), aiming to collect measurements at various relative azimuth angles to the sun. In principle, calibration flights require clear, clean sky conditions above the aircraft, which was a challenging requirement to meet over SWA. As shown in **Fig. 8**, the polarization ratio

602 profiles measured by the ATR lidar indicated an aerosol layer at 4 km AMSL, which
603 was also spotted by pilots and detected with in-situ aerosol measurements.
604
605 The presence of the thick aerosol layer led to the decision to climb after completing
606 the first box pattern. However, towards the end of the flight, frequent clouds and
607 aerosol were present over SWA (**Figure 9)**, making both calibration and radiation
608 closure studies challenging. During the aircraft campaign, dust was forecasted by
609 the European center for Medium-range Weather Forecasts Copernicus Atmosphere
610 Monitoring Service-Integrated Forecasting System to be mainly north of 8°N (latitude
611 of Savè) and southward transport over the Soudanian zone was clearly modulated
612 by major synoptic-scale features (Knippertz et al., 2017).
613
614 **Figure 10** shows an example of a radiation closure at the aircraft altitude, using
615 calibrated upwelling and downwelling irradiances in the shortwave (SW) and
616 longwave (LW) spectral region from the flight in **Fig. 8**. We compare measured
617 irradiances with those calculated from radiative transfer, using atmospheric profiles
618 from the ERA-Interim reanalysis and cloud properties from SEVIRI as input. Calculated
619 irradiances calculated using the Suite Of Community RAdiative Transfer codes based
620 on Edwards and Slingo (SOCRATES, Edwards and Slingo, 1996). Overall, the
621 agreement between measured and calculated irradiances appears reasonable for
622 the LW, but there are clear discrepancies in the SW. The calculated downwelling
623 irradiance is systematically larger than the measurements, which may be due to
624 overlying aerosol layers that have not been included in radiative transfer calculations.
625 In the upwelling direction, the calculated SW irradiance agrees with measurements
626 reasonably well in the first part of the aircraft transect, but tends to be 50 W m^{-2}
627 smaller after 1105 UTC, suggesting that clouds from SEVIRI retrievals are not bright

enough. These hypothesized sources of errors will be investigated further using cloud and aerosol properties from the aircraft and ground sites and the GERB instrument (as shown in **Fig. 9** and described in Sect. 6).

d. Low-level clouds on 7–8 July 2016

In order to demonstrate the spatio-temporal evolution of nocturnal LLCs and their relation to the horizontal wind field, we select an IOP in which nocturnal LLCs develop at all three supersites (IOP 8, 7–8 July 2016). On this day, the large-scale conditions in the investigation area are characterized by about 1000 m deep south-westerly monsoon flow and the AEJ above, as evident from the radiosonde network data (see Section 4, **Fig. 3**). In the afternoon of 7 July, a moderate monsoon flow of about 3 m s^{-1} prevails. The transition layer from the southwesterly monsoon flow to the easterly wind above ranges from about 1000 to 1500 m AGL. The wind speed of the AEJ increases from south to north, e.g., the UHF wind profiler at Savè detects the AEJ at about 3500 m AGL with 15 m s^{-1} in strength.

The comparison of the occurrence and base height of the LLCs at the three supersites reveals a considerable variability (**Figure 11**). In Ile-Ife, first LLCs were observed around 2100 UTC (**Fig. 11c)**. In Kumasi, the first LLCs are detected at 2030 UTC, becoming continuous after 2130 UTC (**Fig. 11a**). In Savè, LLCs developed around midnight (**Fig. 11b**). During the night, the cloud base at Ile-Ife drops from 300 m AGL at 2100 UTC to around 30 m AGL at 0300 UTC. At Savè, the cloud base is rather constant at about 250 m AGL. At Kumasi the cloud base decreases slightly from about 300 m AGL at 2200 UTC to 200 m AGL in the early morning. The ceilometer data from Kumasi and Savè show that the cloud base starts to rise

654 between 0700 and 0800 UTC (**Fig. 11a, b**). The cloud base starts to rise when the net
655 radiation becomes positive, as seen in energy balance data (not shown). At 1200
656 UTC, when the CBL is well established, the cloud base is at about 700 m AGL at
657 Kumasi and at 800 m AGL at Savè.
658
659 The different evolution of LLCs at the three supersites is also reflected in the net LW
660 radiation, $L_{net} = L\downarrow - L\uparrow$, ($L\downarrow$ denotes the downward and $L\uparrow$ the upward LW radiation,
661 **Fig. 11d**). LLC are accompanied by an increase of the L_{net} to a value of about -10 W
662 m^{-2}. For example, the formation of LLCs at Savè shortly after midnight (**Fig. 11b**) results
663 in an abrupt increase of L_{net} from about -40 to -10 W m^{-2} (**Fig. 11d**). The strong
664 temporal changes of L_{net} in the morning (between 0800 and 1000 UTC) suggest that
665 the clouds are more broken at Kumasi than at Savè and Ile-Ife.
666
667 **Figure 11** also includes information about the horizontal wind field. A nocturnal south-
668 westerly LLJ forms at all three sites. Schrage and Fink (2012) pointed to the important
669 contribution of LLJs on LLC formation. While the maximum wind speed is rather similar
670 at all sites (around 8–10 m s^{-1}), considerable differences occur in its onset time and
671 duration. At Ile-Ife, a LLJ forms after 1900 UTC and is more or less continuous until
672 around 0800 UTC (**Fig. 11c**). The LLJ at Savè forms 2 hours later, i.e., at 2100 UTC, and
673 becomes deeper in the course of the night (**Fig. 11b**). In Kumasi, a distinct LLJ exists
674 at midnight and 0300 UTC and strongly weakens until 0600 UTC (**Fig. 11a**). At all sites,
675 surface-based heating after sunrise causes vertical mixing and the dissolution of the
676 LLJ. This process occurs parallel to the rise of the cloud base, as best seen at Savè
677 (**Fig. 11b**).
678

679 The comprehensive dataset will be used for analysis of statistics for the whole period
680 as well as investigating individual cases with and without LLCs to identify processes
681 relevant to the diurnal cycle of LLCs and to study the impact of LLC on the CBL
682 conditions.
683
684 *e. BB aerosol plume on 13 July 2016*
685
686 The post-onset period was most favorable to the observation of BB aerosol plumes
687 from the southern hemisphere over the DACCIWA region (Knippertz et al. 2017). On
688 13 July 2016, an anticyclonic vortex traveling over the Gulf of Guinea led to the
689 transport of a massive BB plume originating from Central Africa. The Falcon 20 and
690 ATR 42 conducted flights in the morning (0918–1242 UTC) and afternoon (1225–1551
691 UTC), respectively, which enabled sampling the aged BB plume at different times
692 and in different locations (**Figure 12**). During these flights, the instruments observed
693 the highest CO and organic aerosol concentrations as well as aerosol extinction
694 coefficient values of the entire aircraft detachment period.
695
696 **Figure 13** shows the vertical profile of aerosol number concentration and submicron
697 non-refractory aerosol mass concentration (NR-PM_1) acquired on-board both the ATR
698 and the Falcon. The NR-PM_1 measured by the Aerosol Mass Spectrometers (AMS) on
699 both aircraft shows a significant enhancement between 1.5 and 4.5 km AMSL
700 indicative of the presence of a BB plume. The Falcon-observed profile shows a single
701 layer, while the ATR-observed profiles exhibits a two-layer structure with NR-PM_1 values
702 peaking at 40 µg m^{-3} at 2.5 km AMSL and nearly 100 µg m^{-3} at 3.8 km AMSL (the former
703 AMS is still undergoing calibration such that values in **Figure 13** are in arbitrary units).
704 Unexpectedly, high values of NR-PM_1 concentrations (~20 µg m^{-3}) were observed

above the top of the marine boundary layer. The differences may be related to the fact that the aircraft did not sample the plume in the exact same location, with the ATR 42 operating farther to the west (see **Fig. 12**) or to the temporal evolution of the BB plume.

Aerosol number concentration was measured on-board the Falcon using a Condensation Particle Counter (CPC) and an Ultra-High Sensitivity Aerosol Spectrometer (UHSAS), measuring particles with a diameter larger than 10 nm and 100 nm, respectively. The enhanced concentrations observed between 2 and 4 km AMSL with the CPC and the UHSAS (co-located with the AMS) and the agreement between the two instruments are an indication that the aerosol population is strongly dominated by the accumulation mode, in good agreement with previous measurements of BB aerosols (e.g., Brito et al. 2014). Refractory Black Carbon (rBC) measurements, performed using the Single Particle Soot Photomer (SP2) on-board the ATR 42, provide further insight into the chemical composition of BB plumes at different altitudes. The rBC profile reveals two concentration maxima in biomass burning layers, concurrently with enhanced concentrations of Organic Aerosols (OA) and CO (**Figure 14**). Interestingly, higher concentrations of both OA and CO were observed in the upper plume around 4 km AMSL, while rBC concentrations were similar in both layers. Since forest fires are important emission sources for OA, CO, and rBC, the contrast in rBC/OA and rBC/CO ratios between the two BB layers likely relates to different processes affecting the air masses during their transport (e.g., Pan et al., 2011; Jolleys et al, 2015).

These observations have major implications for understanding the climatic effects of biomass burning aerosols, since the aging processes take place over large spatial and

731 temporal scales. Future research specifically targeting aerosol microphysical and
732 chemistry processes is therefore essential to understand the cause of this variability and
733 provide reliable parameterisations of BB processes. In addition to providing a wealth of
734 observations to validate and improve atmospheric chemistry models, the data from
735 these flights will be used to assess the impact of long-range transport of BB aerosols
736 on air quality in the DACCIWA region compared to city emissions. They will also serve
737 to improve our understanding of the radiative impact of BB aerosols on the formation
738 and life cycle of mid-level clouds, which was the primary objective of the MICWA
739 operation conducted with the ATR on 13 July 2016.
740

741 **8. Conclusions and outlook**

742

743 The DACCIWA project organized an ambitious field campaign over SWA (Ivory Coast,
744 Ghana, Togo, Benin, and Nigeria) during June-July 2016, bringing together over 200
745 people from European and African institutions. The campaign included aircraft,
746 ground-based, urban, and radiosounding components to improve our knowledge of
747 the physical processes involved in the low-level cloud life cycle in the complex
748 chemical environment of SWA, and the implication for weather, climate, and air
749 pollution. During this detachment, DACCIWA scientists conducted a total of 155 flight
750 hours using three aircraft, acquired over 1100 hours of data from three ground
751 supersites, and launched over 770 radiosondes. An unprecedented wealth of in-situ
752 and remote-sensing observations was obtained over SWA using state-of-the-art
753 instruments, which were implemented timely thanks to the genuine cooperation
754 between European and African partners. Moreover, capacity building efforts were
755 undertaken in Benin, Ghana, and Ivory Coast at several supersites and radiosonde
756 stations.

A number of "firsts" were achieved during the DACCIWA field campaign:

1. documentation of the diurnal cycle of stratus, stratocumulus, and cumulus over SWA using three aircraft with very similar payloads measuring atmospheric dynamics / thermodynamics, gas phase chemistry, aerosols, and clouds in coordination with a wide range of ground-based instrumentation and the densest radiosounding network ever;
2. systematic mapping of pollution around and downstream Accra and Lomé plus some occasional measurements around Abidjan and Cotonou in coordination with surface-based urban emission measurements;
3. documentation of atmospheric dynamics / thermodynamics and composition in the vicinity of mid-level clouds;
4. observations to link atmospheric conditions in the region of coastal upwelling with the life cycle of inland stratocumulus;
5. dedicated aircraft-based radiation calibration and closure effort to improve satellite based radiation products specifically over SWA in a contrasted and complex chemical environment,
6. seven weeks of continuous high-quality in situ and remote sensing measurements in SWA, invaluable for process studies and model evaluation.

Finally, observations acquired during the DACCIWA field campaign will undoubtedly contribute to improve climate, weather, and air quality models as well as satellite retrievals, which are needed to support policies towards a more sustainable development for the region. This ambitious goal can hardly be achieved by researchers directly involved in the DACCIWA campaign alone. Therefore, all quality-checked data, along with necessary meta-information, will be made available in the

783 DACCIWA database after a two-year embargo period (May 2019, at the latest), but
784 are available for immediate use for associated partners. The DACCIWA data base is
785 hosted by the Base de l'Afrique – Beyond AMMA Base (BAOBAB) website
786 (http://baobab.sedoo.fr) that allows accessing data from AMMA and several other
787 West African field activities. The DACCIWA project has partly supported this website
788 and it is hoped that this article contributes to a wide usage of its rich data content.
789

790 **Acknowledgements**

791

792 The DACCIWA project has received funding from the European Union Seventh
793 Framework Programme (FP7/2007-2013) under grant agreement no. 603502. The
794 European Facility for Airborne Research (EUFAR, http://www.eufar.net/) also
795 supported the project through the funding of 3 Transnational Activity projects:
796 MICWA, APSOWA, and OLACTA (for additional details, see
797 http://www.eufar.net/media/uploads/documents/filer_public/8a/93/8a93ecc5-
798 c9b4-4536-8b9c-daa541ada8fc/eufar_newsletter_sept2016_issue17.pdf). The Centre
799 National d'Etudes Spatiales (CNES) also provided financial support to the project. The
800 authors are grateful to the numerous colleagues from European and African
801 institutions that have contributed to the DACCIWA field campaign. We have listed
802 them in the Supplement to this overview paper. The Service des Avions Français
803 Instrumentés pour la Recherche en Environnement (SAFIRE, a joint entity of CNRS,
804 Météo-France and CNES and operator of the ATR 42), the British Antarctic Survey
805 (BAS, operator of the Twin Otter) and the Deutsches Zentrum für Luft- und Raumfahrt
806 (operator of the Falcon 20) are thanked for their support. The authors would also like
807 to thank Gregor Pante for help with producing Fig. 3. We are thankful to the

anonymous referees and the Editor for having taken the time to review the paper and make suggestions on how to improve it.

References

Adler, B., N. Kalthoff, and L. Gantner, 2017: The life cycle of nocturnal low-level clouds over southern West Africa analysed using high-resolution simulations. *Atmos. Chem. Phys.*, doi:10.5194/acp-2016-842.

Bourgeois, Q., A. M. L. Ekman, M. R. Igel, and R. Krejci, 2016: Ubiquity and impact of thin mid-level clouds in the tropics. *Nature Communications*, **7,** DOI: 10.1038/ncomms12432

Brito, J., L. V. Rizzo, W. T. Morgan, H. Coe, B. Johnson, J. Haywood, K. Longo, S. Freitas, M. O. Andreae, and P. Artaxo, 2014: Ground-based aerosol characterization during the South American Biomass Burning Analysis (SAMBBA) field experiment, *Atmos. Chem. Phys.,* **14,** 12069–12083.

Edwards, J. M., and A. Slingo, 1996: Studies with a flexible new radiation code. I: Choosing a configuration for a large-scale model. *Quart. J. Roy. Meteor. Soc.,* **122,** 689–720.

Fink, A. H., D. G. Vincent, and V. Ermert, 2006: Rainfall Types in the West African Soudanian Zone during the Summer Monsoon 2002. *Mon. Wea. Rev.,* **134,** 2143-2164.

Fink A. H., A. Agustí-Panareda, D. J. Parker, J-B. Ngamini, E. Afiesimama, A. Beljaars, O.

834 Bock, M. Christoph, F. Didé, C. Faccani, N. Fourrié, F. Karbou, J. Polcher, Z. Mumba, M.
835 Nuret, S. Pohle, F. Rabier, A. M. Tompkins, and G. Wilson, 2011: Operational
836 meteorology in West Africa: observational networks, weather analysis and
837 forecasting. *Atmos. Sci. Let.,* **12,** 135–141.
838
839 Hannak, L., P. Knippertz, A. H. Fink, A. Kniffka, and G. Pante, 2017): Why do global
840 climate models struggle to represent low-level clouds in the West African summer
841 monsoon? *J. Climate,* **30,** 1665–1687.
842
843 Hill, P. G., R. P. Allan, J. C. Chiu, and T. H. M. Stein, 2016: A multi-satellite climatology
844 of clouds, radiation, and precipitation in southern West Africa and comparison to
845 climate models, *J. Geophys. Res. Atmos.,* **121,** 10,857-10,879.
846
847 IPCC, 2013: Climate Change 2013: The Physical Science Basis. Contribution of
848 Working Group I to the Fifth Assessment Report of the Intergovernmental Panel on
849 Climate Change [Stocker, T.F., D. Qin, G.-K. Plattner, M. Tignor, S.K. Allen, J. Boschung,
850 A. Nauels, Y. Xia, V. Bex and P.M. Midgley (eds.)]. Cambridge University Press,
851 Cambridge, United Kingdom and New York, NY, USA, 1535 pp.
852
853 Jolleys, M. D., H. Coe, G. McFiggans, J. W. Taylor, S. J. O'Shea, M. Le Breton, SL J.-B.
854 Bauguitte, S. Moller, P. Di Carlo, E. Aruffo, P. I. Palmer, J. D. Lee, C. J. Percival, and M.
855 W. Gallagher, 2015: Properties and evolution of biomass burning organic aerosol from
856 Canadian boreal forest fires, *Atmos. Chem. Phys.,* **15,** 3077-3095.
857
858 Knippertz, P., A. H. Fink, A. Deroubaix, E. Morris, F. Tocquer, M. Evans, C. Flamant, M.
859 Gaetani, C. Lavaysse, C. Mari, J. H. Marsham, R. Meynadier, A. Affo-Dogo, T. Bahaga,

F. Brosse, K. Deetz, R. Guebsi, I. Latifou, M. Maranan, P. D. Rosenberg, and A. Schlueter, 2017: A meteorological and chemical overview of the DACCIWA field campaign in West Africa in June–July 2016, *Atmos. Chem. Phys. Disc.*, doi:10.5194/acp-2017-345

Knippertz, P., M. Evans, P. R. Field, A. H. Fink, C. Liousse, and J. H. Marsham, 2015b: The possible role of local air pollution in climate change in West Africa. *Nature Clim. Change,* doi:10.1038/NCLIMATE2727.

Knippertz P., H. Coe, C. Chiu, M. J. Evans, A. H. Fink, N. Kalthoff, C. Liousse, C. Mari, R. Allan, B. Brooks, S. Danour, C. Flamant, O. O. Jegede, F. Lohou and J. H. Marsham, 2015a: The DACCIWA project: Dynamics-aerosol-chemistry-cloud interactions in West Africa, *Bull. Amer. Meteorol. Soc.*, **96,** 1451-1460.

Kuettner, J. P., 1974: General description and central program of GATE, *Bull. Am. Meteorol. Soc.,* **55,** 712–719.

Lebel, T., D. J. Parker, C. Flamant, B. Bourlès, B. Marticorena, E. Mougin, C. Peugeot, A. Diedhiou, J. M. Haywood, J. B. Ngamini, J. Polcher, J. L. Redelsperger, and C. D. Thorncroft, 2010: The AMMA field campaigns: Multiscale and multidisciplinary observations in the West African region, *Q. J. R. Meteorol. Soc.,* **136(s1)**, 8–33.

Leduc-Leballeur, M., G. De Coëtlogon, and L. Eymard, 2013 : Air-sea interaction in the gulf of Guinea at intraseasonal time-scales : wind bursts and coastal precipitation in boreal spring. *Quart. J. Roy. Meteor. Soc.,* **139,** 387-400.

885 Mann, J. A. L., J. C. Chiu, R. J. Hogan, E. J. O'Connor, T. S. L'Ecuyer, T. H. M. Stein, and
886 A. Jefferson, 2014: Aerosol impacts on drizzle properties in warm clouds from ARM
887 Mobile Facility maritime and continental deployments, *J. Geophys. Res. Atmos.,* **119,**
888 4136-4148.
889
890 Mülmenstädt, J., O. Sourdeval, J. Delanoë, and J. Quaas, 2015: Frequency of
891 occurrence of rain from liquid-, mixed-, and ice-phase clouds derived from A-Train
892 satellite retrievals, *Geophys. Res. Lett.,* **42,** 6502–6509.
893
894 Pan, X. L., Y. Kanaya, Z. F. Wang, Y. Liu, P. Pochanart, H. Akimoto, Y. L. Sun, H. B.
895 Dong, J. Li, H. Irie, and M. Takigawa, 2011: Correlation of black carbon aerosol and
896 carbon monoxide in the high-altitude environment of Mt. Huang in Eastern China,
897 *Atmos. Chem. Phys.,* **11,** 9735-9747.
898
899 Parker, D. J., A. H. Fink, S. Janicot, J-B. Ngamini, M. Douglas, E. Afiesimama, A. Agusti-
900 Panareda, A. Beljaars, F. Dide, A. Diedhiou, T. Lebel, J. Polcher, J.-L. Redelsperger, C.
901 Thorncroft, and G. A. Wilson, 2008: The AMMA radiosonde program and its
902 implications for the future of atmospheric monitoring over Africa. *Bull. Amer. Meteor.*
903 *Soc.,* **89,** 1015–1027.
904
905 Redelsperger, J.-L., C. D. Thorncroft, A. Diedhiou, T. Lebel, D. J. Parker, and J. Polcher,
906 2006: African Monsoon Multidisciplinary Analysis: An international research project
907 and field campaign. *Bull. Am. Meteorol. Soc.*, **87**, 1739 – 1746.
908

909 Schrage, J. M., and A. H. Fink, 2012: Nocturnal Continental Low-Level Stratus over
910 Tropical West Africa: Observations and Possible Mechanisms Controlling Its Onset,
911 *Monthly Wea. Rew.,* 140, 1794-1809.
912
913 Schuster, R., A. H. Fink, and P. Knippertz, 2013: Formation and maintenance of
914 nocturnal low-level stratus over the southern West African monsoon region during
915 AMMA 2006. *J. Atmos. Sci.,* **70,** 2337–2355.
916
917 Stein, T. H. M., D. J. Parker, J. Delanoë, N. S. Dixon, R. J. Hogan, P. Knippertz, R. I.
918 Maidment, and J. H. Marsham, 2011: The vertical cloud structure of the West African
919 monsoon: a 4 year climatology using CloudSat and CALIPSO. *J. Geophys. Res.*
920 *Atmos.,* **116.** 2156–2202.
921
922 Tompkins, A. M. and A. A. Adebiyi, 2012: Using CloudSat cloud retrievals to
923 differentiate satellite-derived rainfall products over West Africa, *J. Hydrometeor.,* **13,**
924 1810-1816.
925
926 van der Linden, R., A. H. Fink, and R. Redl, 2015: Satellite-based climatology of low-
927 level continental clouds in southern West Africa during the summer monsoon season,
928 J. Geophys. Res. Atmos., **120,** 1186-1201.
929
930 van Zanten, M. C., B. Stevens, G. Vali, and D. L. Lenschow, 2005: Observations of
931 drizzle in nocturnal marine stratocumulus, *J. Atmos. Sci.,* **62,** 88–106.
932
933
934

935 **List of Tables**

936

937 **Table 1**: Top: Overview of the timeline of the DACCIWA campaign and its
938 components. The DACCIWA radiosounding campaign (orange) took place between
939 11 June and 31 July 2016 (**Figures S and S3**), while the ground-based campaign
940 (yellow) took place between 14 June and 30 July 2016. Intensive observation periods
941 (IOPs) conducted at the ground-based supersites prior and after the aircraft
942 campaign (29 June-16 July 2016) are indicated in green (numbers correspond to IOP
943 numbers). Bottom: Timeline of the aircraft campaign with duration of the urban
944 campaigns in Abidjan and Cotonou, and the list of ground-based supersite IOPs
945 conducted during this period. Colored crosses indicate when the airborne platforms
946 (ATR42, Falcon 20, Twin Otter) flew in the vicinity of the supersites. The table also
947 provides a summary of satellite overpasses, including the Moderate Resolution
948 Imaging Spectroradiometer (MODIS) aboard Terra and Aqua, the Visible Infrared
949 Imaging Radiometer Suite (VIIRS) aboard Suomi National Polar-orbiting Partnership
950 (NPP), the Megha-Tropiques, and the core instruments of the Global Precipitation
951 Mission (GPM). Colors represent various platforms, while sizes of the filled circles
952 provide an indication of whether the distance and the time between the aircraft
953 track and the nearest satellite pixel meet the given thresholds.

954

955 **Table 2**: Aircraft information and science flight hours completed.

956

957 **Table 3:** List of DACCIWA campaign and NIMET operational radiosonde stations,
958 operating agency, sonde type and launch times. Station in italics are operational
959 upper-air stations. ASECNA: Agence pour la Sécurité de la Navigation Aérienne en
960 Afrique et à Madagascar; SODEXAM: Société de Développement et d'Exploitation

961 Aéroportuaire et Maritime; DNM: Direction National de la Météorologie; NIMET:
962 Nigerian Meteorological Agency; IC: Ivory Coast. UFHB: Université Félix Houphouët-
963 Boigny; KNUST: Kwame Nkrumah University of Science and Technology; GMET:
964 Ghana Meteorological Agency; KIT: Karlsruhe Institute of Technology; UPS: Université
965 Paul Sabatier.
966
967
968
969

970 **List of Figures**

971

972 **Figure 1**: Geographical overview with key landmarks for the DACCIWA campaign
973 operations overlain on topography. The yellow symbols represent radiosounding
974 stations and the blue symbols are ground-based supersites. The yellow-circled blue
975 symbols indicate supersites with balloon sounding capability. The green symbol shows
976 the location of the aircraft operation base (linked with an aircraft schematic). The oil
977 and gas fields locations off-shore of Ghana and Ivory Coast are symbolized with oils
978 rig schematic.

979

980 **Figure 2**: Upper left panel: latitude-longitude representation of flight tracks of all
981 aircraft (50 in total) over SWA between 29 June and 16 July 2016: The DLR Falcon 20
982 flight tracks (12 flights) are in green, the SAFIRE ATR 42 flight tracks (20 flights) are in
983 red, and the BAS Twin Otter tracks (18 flights) are in blue. Upper right panel: Altitude-
984 latitude representation of all aircraft flight tracks. Lower left panel: Altitude-longitude
985 representation of all aircraft flight tracks.

986

987 **Figure 3**: Time-height diagram showing the evolution of the vertical wind regime at
988 Parakou (Benin) from 09–16 July 2016. Plotted are 6-hourly vertical profiles of zonal
989 wind speed in m s^{-1} (colored raster) and wind barbs with short/long ticks indicating
990 5/10 knots and a filled triangle 50 knots. Thick contour indicates zero zonal wind
991 speed. Vertical resolution is every 25 hPa for wind speed and 300 m for wind barbs
992 (left ordinate) with corresponding altitude in km on the right ordinate. Symbols below
993 the abscissa are according to WMO FM 12 SYNOP coding practices for surface
994 stations (WMO 2010) and denote: mid-level cloud type (C_M), low-level clouds type
995 (C_L), low and mid-level cloud cover in octas (N_{LM}), significant weather (WW), and

996 rainfall in mm (RRR). Rainfall is accumulated over previous 24, 12, and 6 hours for 06,
997 18, and 00/12 UTC observation times, respectively.
998
999 **Figure 4**: Aerosol composition (black carbon –BC, organic carbon –OC, and
1000 particulate organic matter –POM) in ADF (Abidjan domestic fire site), AWB (Abidjan
1001 waste burning site), AT (Abidjan traffic site), and CT (Cotonou traffic site). The inner,
1002 middle, and outer circles indicate ultra-fine (<0.2 μm), fine (0.2-1 μm), and coarse (>
1003 1 μm) particles, respectively. Total aerosol mass in μg m^{-3} is given in brackets
1004
1005 **Figure 5**. Profiles of the aerosol concentration measured by PCASP probes on (a) the
1006 SAFIRE ATR 42 between 0800 and 1100 UTC, (b) the DLR Falcon 20 between 1120 and
1007 1500 UTC, and (c) the BAS Twin Otter between 1600 and 1750 UTC on 5 July 2016. (d)–
1008 (f) same as (a)–(c), but for the cloud droplet number concentration (CDNC). Panels
1009 (g)–(i) show SEVIRI cloud top height taken at times during each research flight (ATR
1010 42, Falcon 20, and Twin Otter, respectively, see text for the times of the flights). Green
1011 areas represent cloud-free regions as ween with SEVIRI.
1012
1013 **Figure 6**. Time-height evolution of backscatter (color-coded) and cloud base height
1014 from ceilometer (black dots) in Savè on 5 July 2016. Cloud bases are observed as the
1015 thin layer of high backscatter.
1016
1017 **Figure 7**. (a) Flight tracks from the three aircraft for flights undertaken on 6 July 2016.
1018 Squares show the DLR Falcon, triangles the SAFIRE ATR, and circles the BAS Twin Otter.
1019 Points are colored by altitude in meters, CO in ppbv, CH_4 in ppbv, and NO_2 in pptv,
1020 all averaged for 60 s (except the CH_4 data from the DLR Falcon, which is averaged
1021 over the 30 s bag sampling period). Also labeled are ABJ = Abidjan, Ivory Coast; TTP

= Takoradi Thermal Power Plant, Ghana; ACR = Accra, Ghana; LOM = Lomé, Togo. (b) Cross sections of latitude vs. altitude for the BAS Twin Otter legs downwind of Accra (from flight tracks within the black dashed line in part (a)). Data is 1 s averaged.

Figure 8. Profiles of raw depolarization ratio (ρ_{raw}, color) measured from the lidar ULICE onboard the SAFIRE ATR42 during flight #21 on 2 July 2016. The lidar data is overlain on terrain elevation (greenish colors). This figure is credited to P. Chazette (LSCE, CEA/CNRS).

Figure 9. (a) Aerosol optical depth at 550 nm retrieved from NPP-SUOMI overpass at 1300 UTC. Note that aerosols over bright surfaces are not available yet in the current operational product. (b) Cloud optical depth, (c) and (d) SW and LW irradiance at the top of the atmosphere, respectively, observed from SEVIRI at 1230 UTC. These are satellite observations close to the end of the flight track shown in **Fig. 8**. The ATR 42 flight track is shown as the purple solid line in all four panels. The DACCIWA focus region is indicated by a dashed box.

Figure 10. Intercomparison between the observed (blue) and the calculated (red, see text for details) downwelling (upper) and upwelling (lower) irradiances in the LW (left) and SW (right) spectral region at the aircraft altitude during the ATR flight on 2 July 2016. Observed irradiances are shown with uncertainty of one standard deviation in light blue shading, estimated from instrumental uncertainty. For SW downwelling irradiances, uncertainty also includes errors in correcting effects of aircraft pitch and roll offsets and radiometer mounting offsets. The associated

uncertainty of one standard deviation in light red shading accounts for temporal and spatial variations in satellite cloud retrievals.

Figure 11: (a)–(c) Horizontal wind vectors (arrows), absolute value of wind speed (color-coded), and cloud base (circles) for the three ground sites Kumasi, Savè, and Ile-Ife, and (d) 1-min averaged net longwave radiation. The triangles in (a)–(c) indicate sunset and sunrise, respectively. In Kumasi the wind is derived from radiosondes and sodar, in Savè it is a composite of sodar and UHF wind profiler data, and in Ile-Ife it is based on sodar data. The cloud base height for Kumasi and Savè is derived from ceilometer data and is based on the algorithm of the manufacturers. For Ile-Ife, the cloud base height is estimated from the relative humidity data measured with tethered radiosondes.

Figure 12. Left column: Latitude-altitude representation of the ATR 42 (top) and Falcon 20 (bottom) flight tracks on 13 July 2016. Right column: Longitude-altitude representation of the ATR 42 (top) and Falcon 20 (bottom) flight tracks. The ATR flight track is color-coded according to AMS-derived NR-PM1 concentrations and the Falcon flight track is color-coded according to UHSAS-derived aerosol concentrations. See text in Section 7e for details.

Figure 13: Profile of measurements from a Condensation Particle Counter (CPC, blue line), an Ultra-High Sensitivity Aerosol Spectrometer (UHSAS, orange line), and Compact Time-of-Flight Aerosol Mass Spectrometer (AMS) on board of the DLR Falcon aircraft (grey line) and ATR42 aircraft (black line) on 13 July 2016. The CPC and UHSAS measure aerosol concentration, with 10 nm cut-off for the former and 100 nm for the latter. AMS data represented here are the sum of the submicron non-refractory

1073 species organics, sulphate, nitrate, ammonium, and chloride (NR-PM_1). Data points
1074 identified as clouds were removed from this analysis. All error bars in this figure
1075 represent the standard error of the mean of the data in the respective size bin, and do
1076 not include systematic errors.
1077
1078 **Figure 14.** Vertical profile of black carbon (BC), organic aerosol (OA) and carbon
1079 monoxide (CO) (left panel) and the BC/CO and OA/CO ratio derived from these
1080 measurements (right panel). The points are mean concentration at each level and the
1081 bars through them are the standard errors.
1082
1083
1084

Tables

Table 1: Top: Overview of the timeline of the DACCIWA campaign and its components. The DACCIWA radiosounding campaign (orange) took place between 11 June and 31 July 2016 (**Figures S2 and S3**), while the ground-based campaign (yellow) took place between 14 June and 30 July 2016. Intensive observation periods (IOPs) conducted at the ground-based supersites prior and after the aircraft campaign (29 June-16 July 2016) are indicated in green (numbers correspond to IOP numbers). Bottom: Timeline of the aircraft campaign with duration of the urban campaigns in Abidjan and Cotonou, and the list of ground-based supersite IOPs conducted during this period. Colored crosses indicate when the airborne platforms (ATR42, Falcon 20, Twin Otter) flew in the vicinity of the supersites. The table also provides a summary of satellite overpasses, including the Moderate Resolution Imaging Spectroradiometer (MODIS) aboard Terra and Aqua, the Visible Infrared Imaging Radiometer Suite (VIIRS) aboard Suomi National Polar-orbiting Partnership (NPP), the Megha-Tropiques, and the core instruments of the Global Precipitation Mission (GPM). Colors represent various platforms, while sizes of the filled circles provide an indication of whether the distance and the time between the aircraft track and the nearest satellite pixel meet the given thresholds.

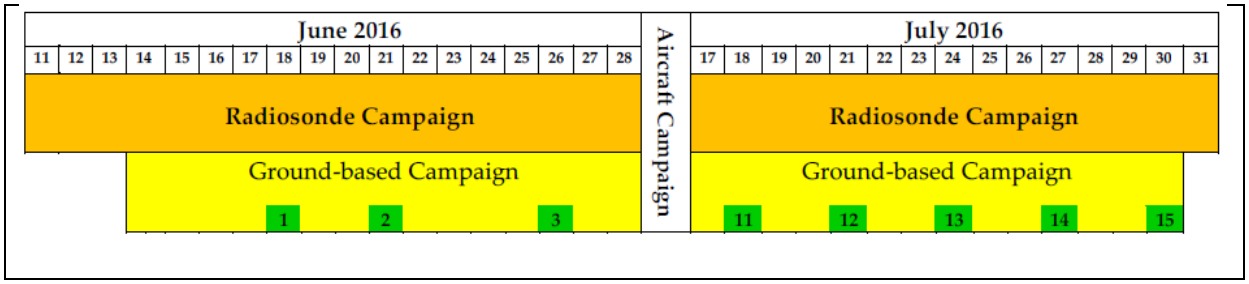

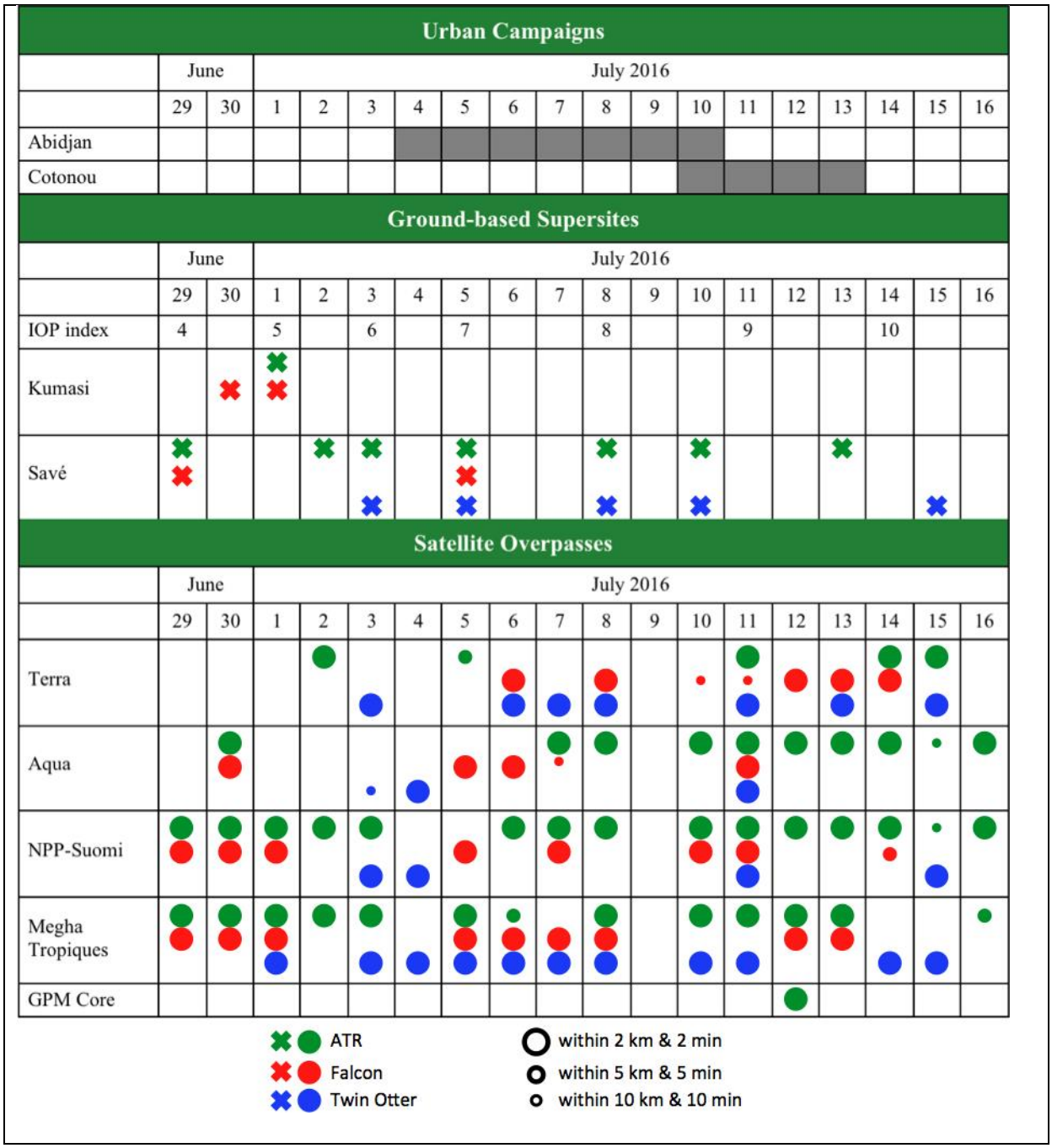
Urban Campaigns
June
July 2016
29 30 1 2 3 4 5 6 7 8 9 10 11 12 13 14 15 16
Abidjan
Cotonou
Ground-based Supersites
June
July 2016
29 30 1 2 3 4 5 6 7 8 9 10 11 12 13 14 15 16
IOP index
4 5 6 7 8 9 10
Kumasi
Savé
Satellite Overpasses
June
July 2016
29 30 1 2 3 4 5 6 7 8 9 10 11 12 13 14 15 16
Terra
Aqua
NPP-Suomi
Megha Tropiques
GPM Core
ATR
Falcon
Twin Otter
within 2 km & 2 min
within 5 km & 5 min
within 10 km & 10 min

1105

1106

1107

1108 **Table 2**: Aircraft information and science flight hours completed.

	SAFIRE ATR 42	DLR Falcon	BAS Twin Otter
Availability in Lomé	27/06 – 16/07	27/06 – 14/07	27/06 – 16/07
Science Flight Hours (incl. EUFAR)	67h49 MICWA*: 12h45 OLACTA§: 10h12	40h34 APSOWA£: 11h06	46h45
Number of science flights	20 MICWA: 3 OLACTA: 3	12 APSOWA: 3	18
Altitude range	200 – 25,000 ft	500 – 34,000 ft	1000 – 10,000 ft
Endurance	3h30	3h30	4h
Range	650 nm	1500 nm	480 nm
Speed	100 m s^{-1}	100 –255 m s^{-1}	47-64 m s^{-1}

1109 *MICWA: MId-level Clouds over West Africa.

1110 §OLACTA: Observing the Low-level Atmospheric Circulation in the Tropical Atlantic.

1111 £APSOWA: Air Pollution from Shipping and Oil platforms of West Africa.

1112

Table 3: List of DACCIWA campaign and NIMET operational radiosonde stations, operating agency, sonde type and launch times. Station in italics are operational upper-air stations. ASECNA: Agence pour la Sécurité de la Navigation Aérienne en Afrique et à Madagascar; SODEXAM: Société de Développement et d'Exploitation Aéroportuaire et Maritime; DNM: Direction National de la Météorologie; NIMET: Nigerian Meteorological Agency; IC: Ivory Coast. UFHB: Université Félix Houphouët-Boigny; KNUST: Kwame Nkrumah University of Science and Technology; GMET: Ghana Meteorological Agency; KIT: Karlsruhe Institute of Technology; UPS: Université Paul Sabatier.

Station (Country)	**WMO No./Mobile TEMP name**	**Lat.**	**Lon.**	**Alt. (m)**	**Operated**	**Sonde**	**Campaign Launch hours UTC**
Abidjan (IC)	*65578*	*5°15'N*	*3°56'W*	*7*	*SODEXAM/ ASECNA/*	*MODEM M10*	*00, 06,12, 18*
Cotonou (Benin)	*65344*	*6°21'N*	*2°23'E*	*5*	*DNM Benin/ ASECNA*	*MODEM M10*	*00, 06,12, 18*
Parakou (Benin)	*BJPAR*	*9°21'N*	*2°37'E*	*392*	*DNM Benin/ ASECNA*	*MODEM M10*	*00, 06,12, 18*

Kumasi (Ghana)	GHKUM	6°40'N	1°33'W	279	Univ. Leeds/ KNUST	Vaisala MW41	06 UTC every day 00,12, 18 UTC IOP days
Savé (Benin)	*LA-Save*	8°00'N	2°26'E	166	UPS/ KIT	MODEM M10	06 UTC every day 00,12, 18 UTC IOP days
Accra (Ghana)	GHACC	5°42'N	0°01'W	84	GMET/KIT	GRAW DFM09	00, 06,09, 12, 18 UTC
Lamto (IC)	IVLAM	6°13N	5°01°W	155	UFHB/ KIT	GRAW DFM09	00, 06,09, 12, 18 UTC
Lagos (Nigeria)	65202	6°33'N	3°20'E	19	NIMET	GRAW DFM 09	12 UTC
Enugu (Nigeria)	65257	6°28'N	7°33'E	137	NIMET	MODEM M10	12 UTC
Abuja (Nigeria)	65125	9°15'N	7°00'E	344	NIMET	VAISALA RS92	12 UTC
Calabar (Nigeria)	65264	4°58'N	8°21'E	63	NIMET	GRAW DFM 09	12 UTC

Figures

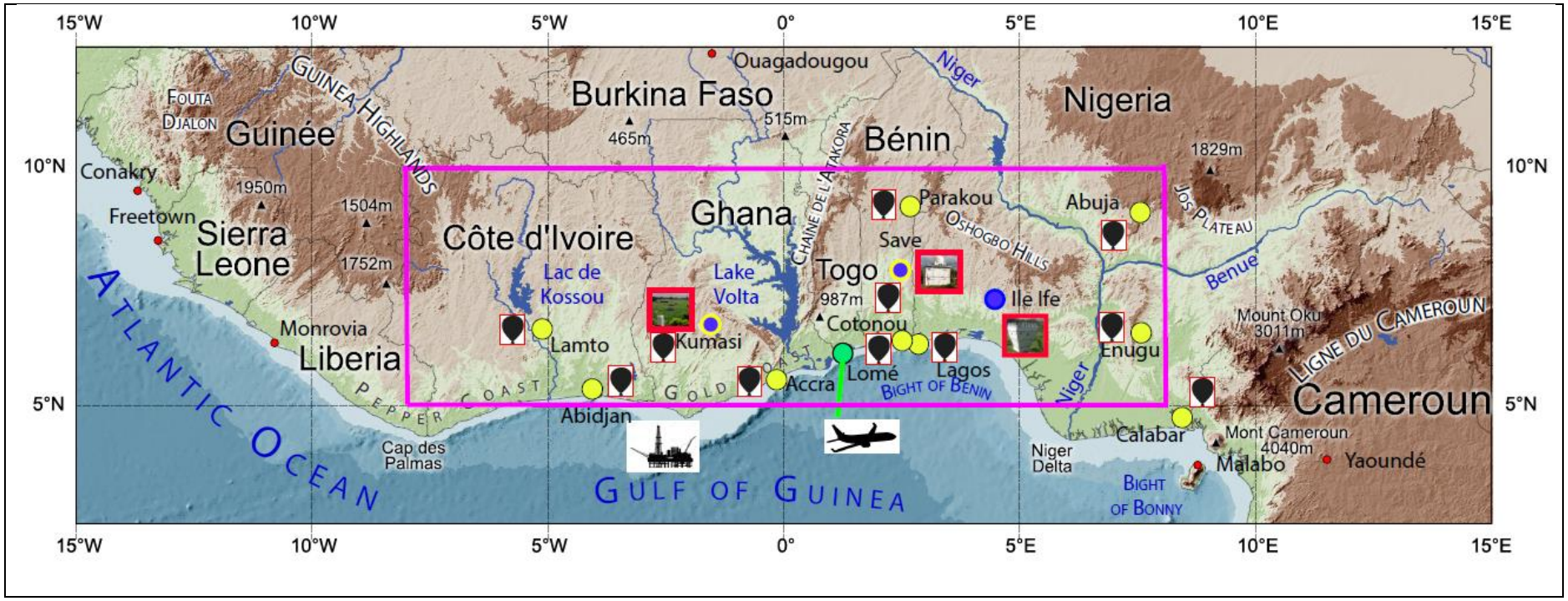

Figure 1: Geographical overview with key landmarks for the DACCIWA campaign operations overlain on topography. The yellow symbols represent radiosounding stations and the blue symbols are ground-based supersites. The yellow-circled blue symbols indicate supersites with balloon sounding capability. The green symbol shows the location of the aircraft operation base (linked with an aircraft schematic). The oil and gas fields locations off-shore of Ghana and Ivory Coast are symbolized with oils rig schematic.

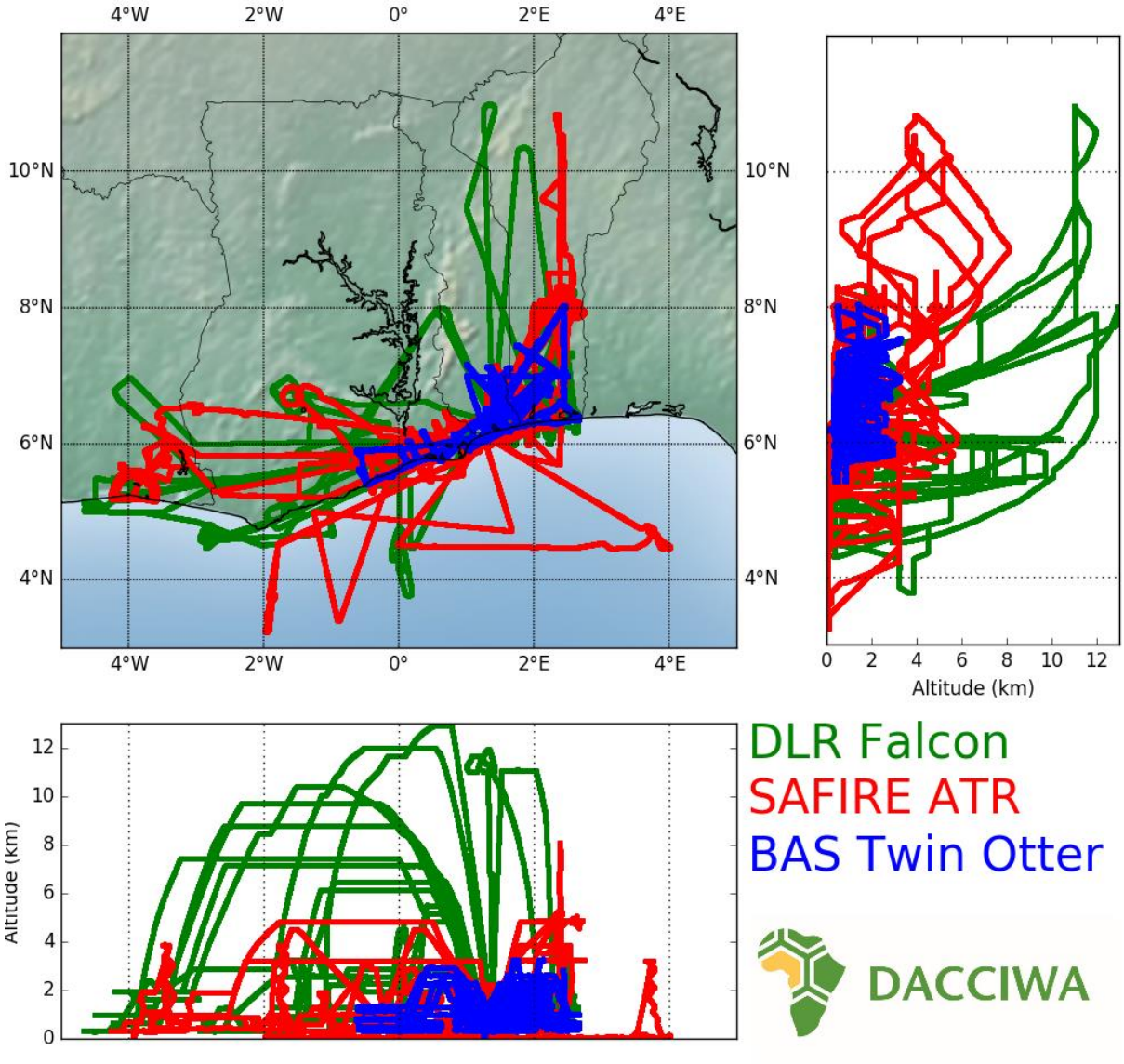

Figure 2: Upper left panel: latitude-longitude representation of flight tracks of all aircraft (50 in total) over SWA between 29 June and 16 July 2016: The DLR Falcon 20 flight tracks (12 flights) are in green, the SAFIRE ATR 42 flight tracks (20 flights) are in red, and the BAS Twin Otter tracks (18 flights) are in blue. Upper right panel: Altitude-latitude representation of all aircraft flight tracks. Lower left panel: Altitude-longitude representation of all aircraft flight tracks.

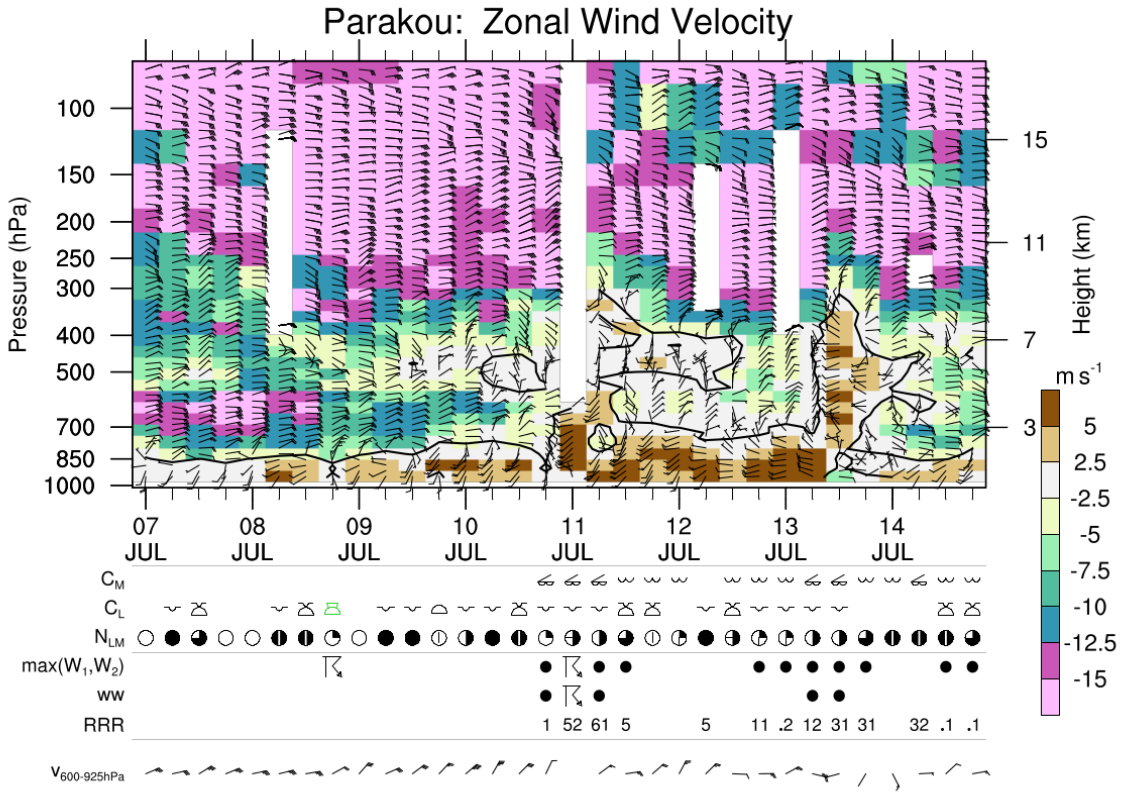

Figure 3: Time-height diagram showing the evolution of the vertical wind regime at Parakou (Benin) from 09–16 July 2016. Plotted are 6-hourly vertical profiles of zonal wind speed in m s^{-1} (colored raster) and wind barbs with short/long ticks indicating 5/10 knots and a filled triangle 50 knots. Thick contour indicates zero zonal wind speed. Vertical resolution is every 25 hPa for wind speed and 300 m for wind barbs (left ordinate) with corresponding altitude in km on the right ordinate. Symbols below the abscissa are according to WMO FM 12 SYNOP coding practices for surface stations (WMO 2010) and denote: mid-level cloud type (C_M), low-level clouds type (C_L), low and mid-level cloud cover in octas (N_{LM}), significant weather (WW), and rainfall in mm (RRR). Rainfall is accumulated over previous 24, 12, and 6 hours for 06, 18, and 00/12 UTC observation times, respectively.

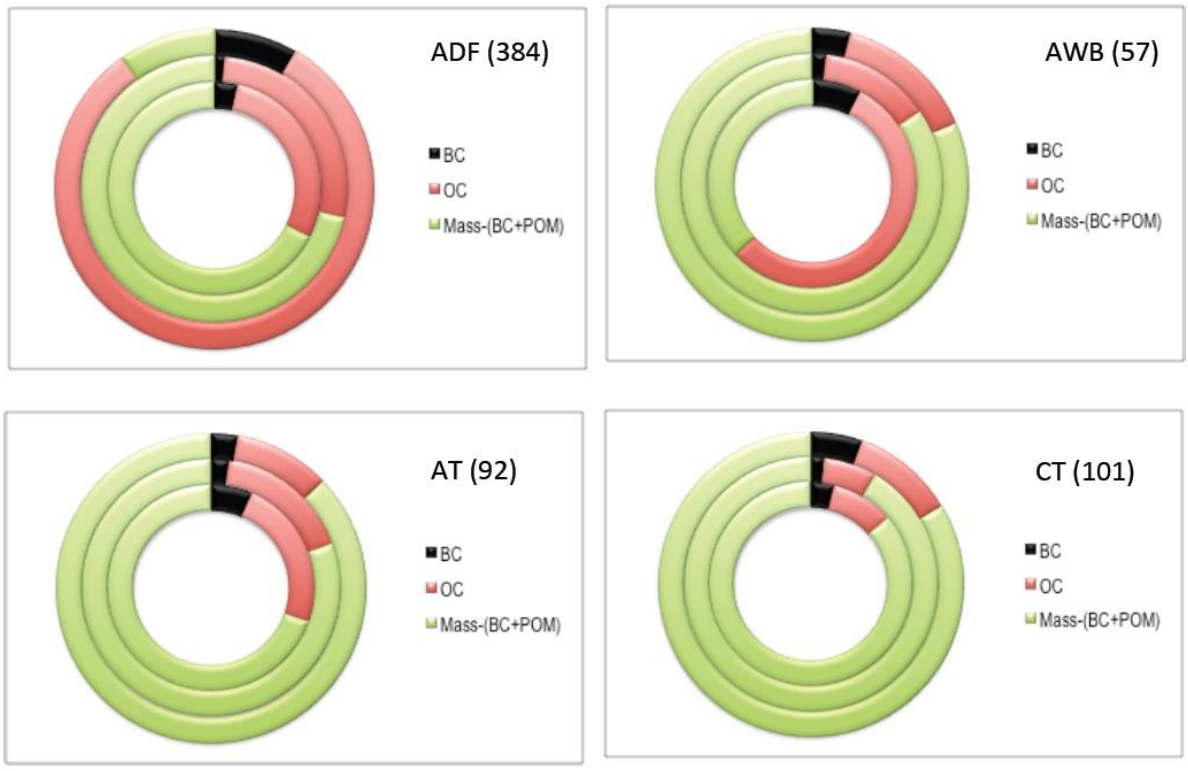

Figure 4: Aerosol composition (black carbon –BC, organic carbon –OC, and particulate organic matter –POM) in ADF (Abidjan domestic fire site), AWB (Abidjan waste burning site), AT (Abidjan traffic site), and CT (Cotonou traffic site). The inner, middle, and outer circles indicate ultra-fine (<0.2 μm), fine (0.2-1 μm), and coarse (> 1 μm) particles, respectively. Total aerosol mass in μg m^{-3} is given in brackets.

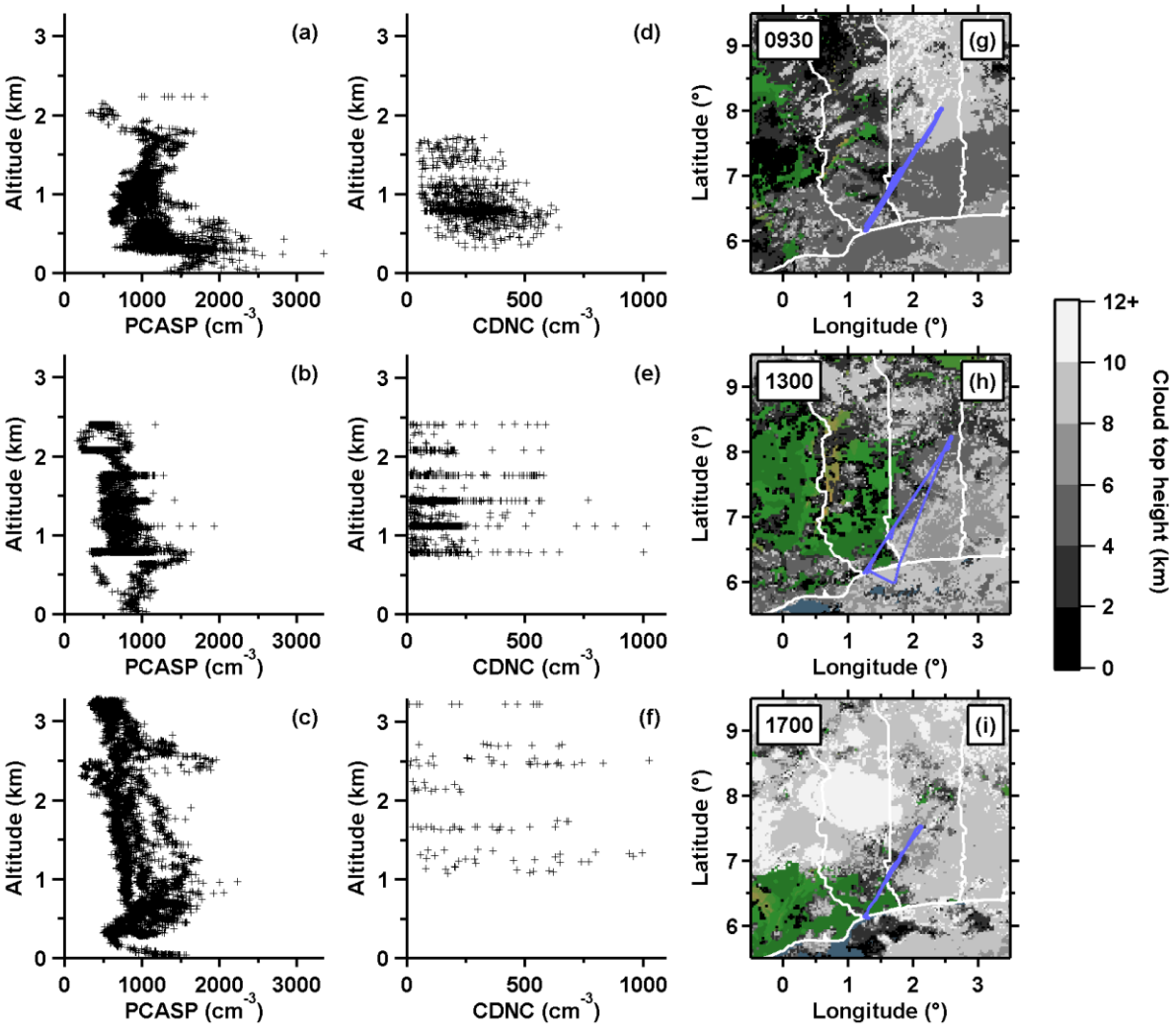

Figure 5. Profiles of the aerosol concentration measured by PCASP probes on (a) the SAFIRE ATR 42 between 0800 and 1100 UTC, (b) the DLR Falcon 20 between 1120 and 1500 UTC, and (c) the BAS Twin Otter between 1600 and 1750 UTC on 5 July 2016. (d)–(f) same as (a)–(c), but for the cloud droplet number concentration (CDNC). Panels (g)–(i) show SEVIRI cloud top height taken at times during each research flight (ATR 42, Falcon 20, and Twin Otter, respectively, see text for the times of the flights). Green areas represent cloud-free regions as seen with SEVIRI.

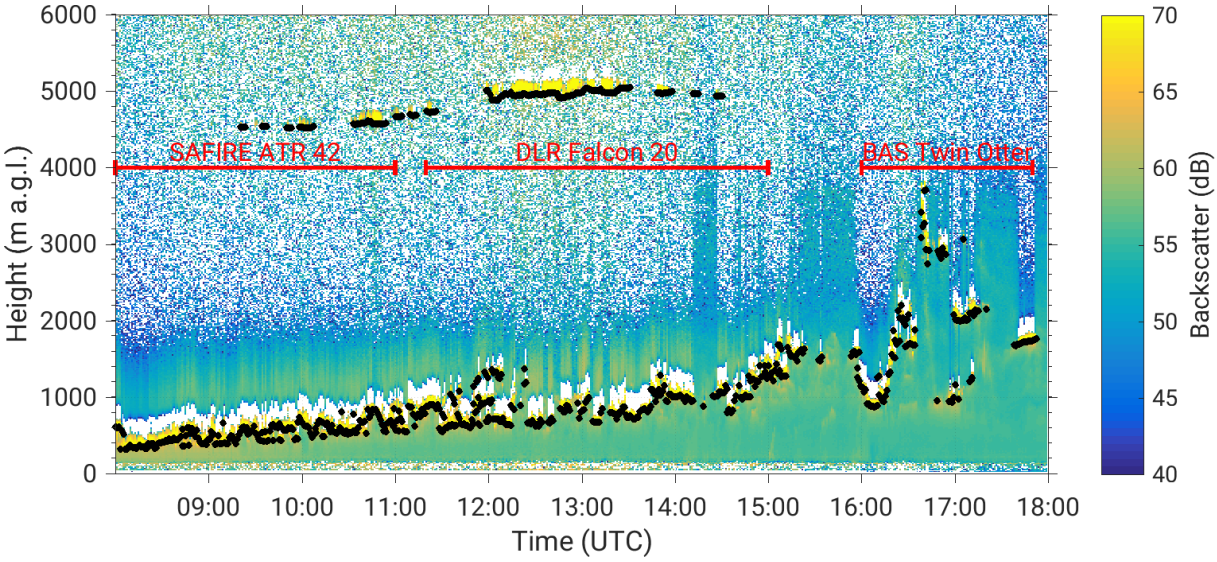

Figure 6. Time-height evolution of backscatter (color-coded) and cloud base height from ceilometer (black dots) in Savè on 5 July 2016. Cloud bases are observed as the thin layer of high backscatter.

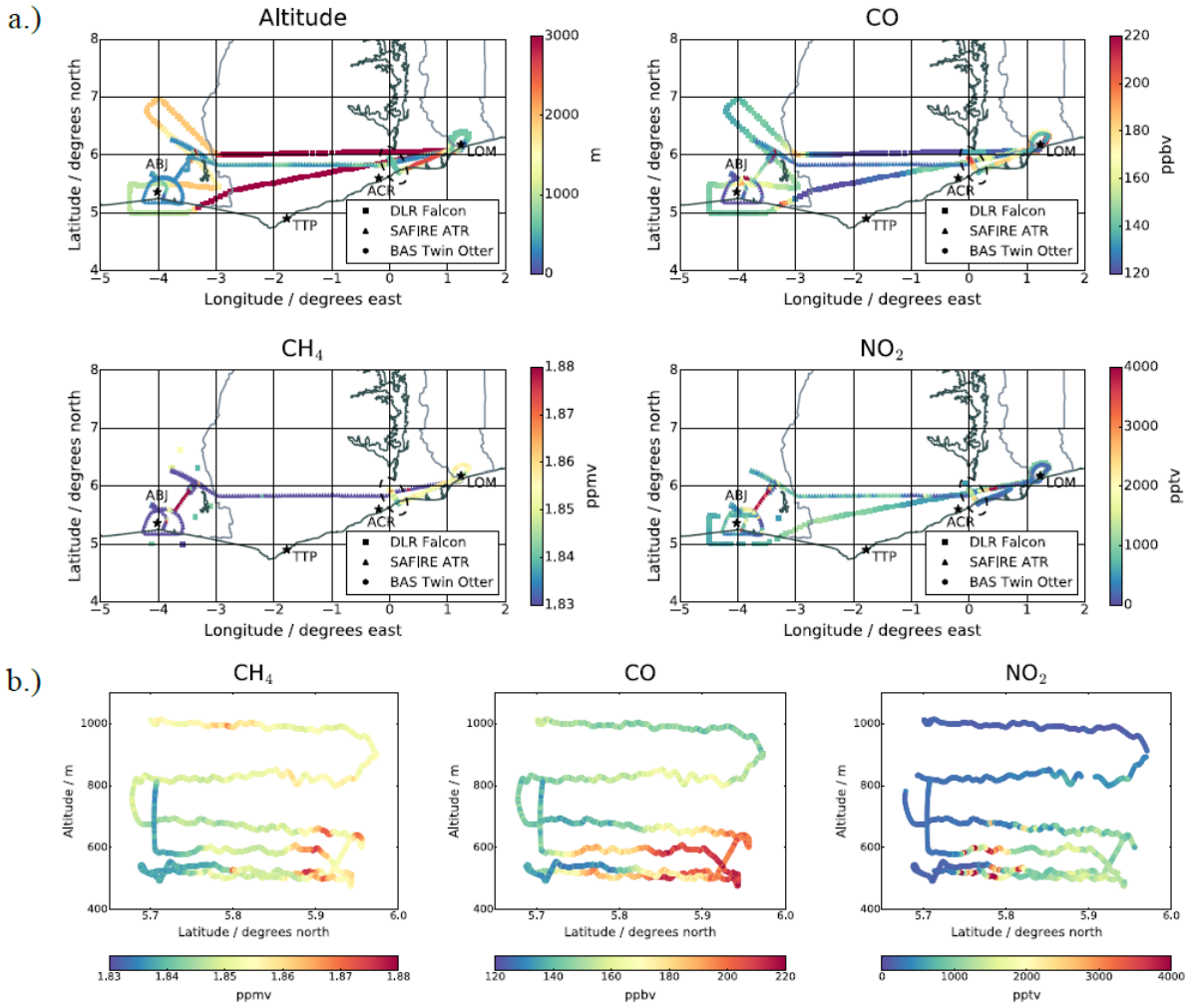

Figure 7. (a) Flight tracks from the three aircraft for flights undertaken on 6 July 2016. Squares show the DLR Falcon, triangles the SAFIRE ATR, and circles the BAS Twin Otter. Points are colored by altitude in meters, CO in ppbv, CH_4 in ppbv, and NO_2 in pptv, all averaged for 60 s (except the CH_4 data from the DLR Falcon, which is averaged over the 30 s bag sampling period). Also labeled are ABJ = Abidjan, Ivory Coast; TTP = Takoradi Thermal Power Plant, Ghana; ACR = Accra, Ghana; LOM = Lomé, Togo. (b) Cross sections of latitude vs. altitude for the BAS Twin Otter legs downwind of Accra (from flight tracks within the black dashed line in part (a)). Data is 1 s averaged.

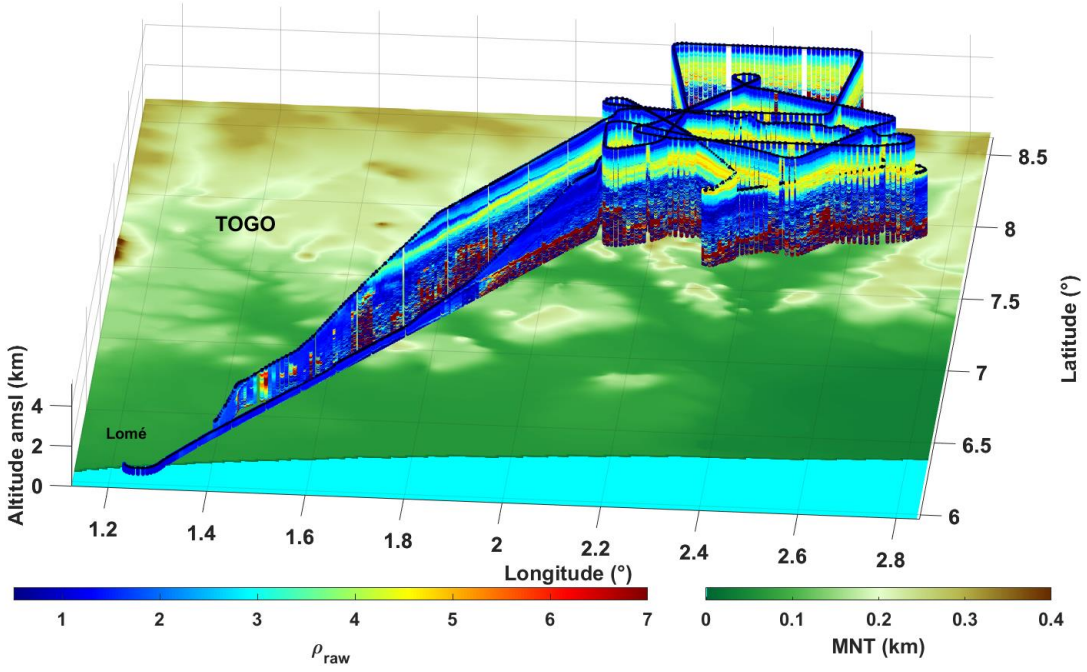

Figure 8. Profiles of raw depolarization ratio (ρ_{raw}, color) measured from the lidar ULICE onboard the SAFIRE ATR42 during flight #21 on 2 July 2016. The lidar data is overlain on terrain elevation (greenish colors). This figure is credited to P. Chazette (LSCE, CEA/CNRS).

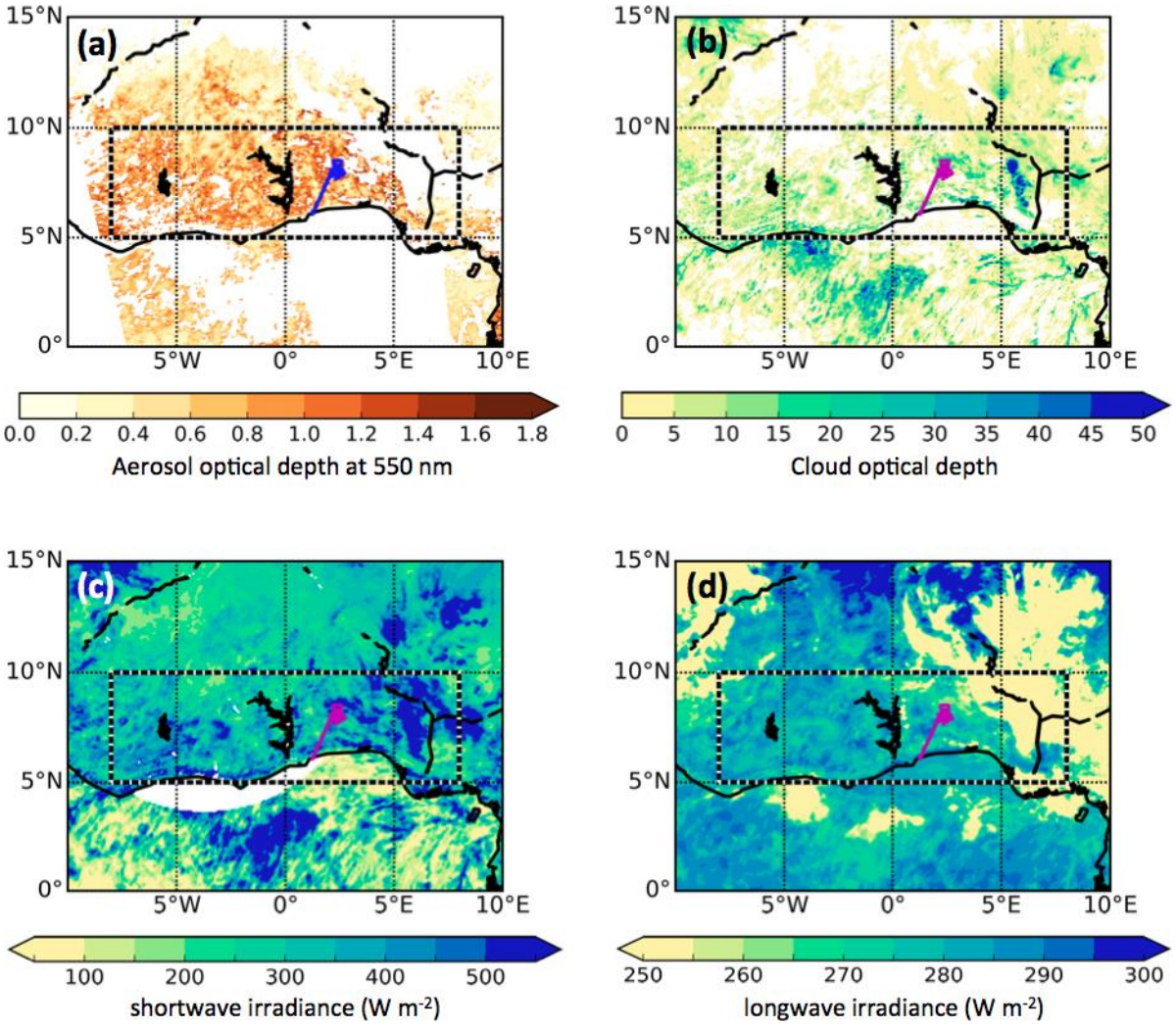

Figure 9. (a) Aerosol optical depth at 550 nm retrieved from NPP-SUOMI overpass at 1300 UTC. Note that aerosols over bright surfaces are not available yet in the current operational product. (b) Cloud optical depth, (c) and (d) SW and LW irradiance at the top of the atmosphere, respectively, observed from SEVIRI at 1230 UTC. These are satellite observations close to the end of the flight track shown in **Fig. 8**. The ATR 42 flight track is shown as the purple solid line in all four panels. The DACCIWA focus region is indicated by a dashed box.

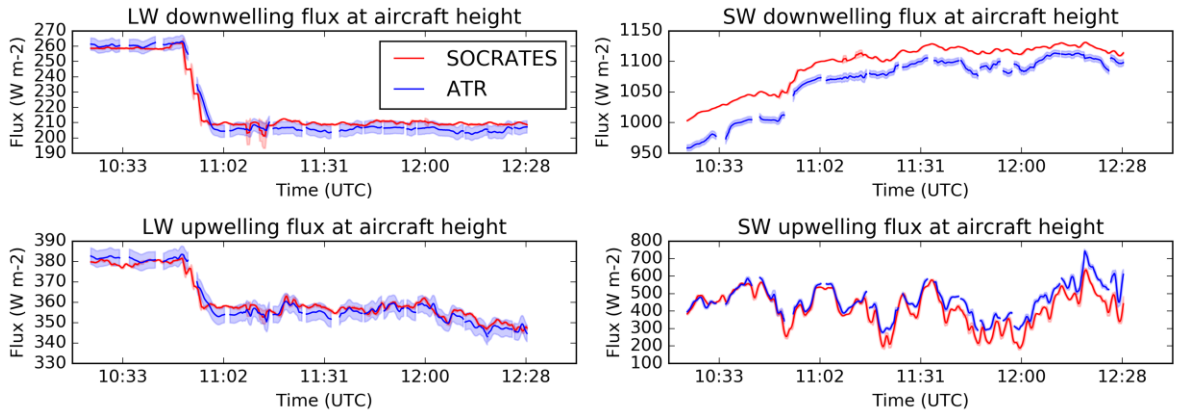

Figure 10. Intercomparison between the observed (blue) and the calculated (red, see text for details) downwelling (upper) and upwelling (lower) irradiances in the LW (left) and SW (right) spectral region at the aircraft altitude during the ATR flight on 2 July 2016. Observed irradiances are shown with uncertainty of one standard deviation in light blue shading, estimated from instrumental uncertainty. For SW downwelling irradiances, uncertainty also includes errors in correcting effects of aircraft pitch and roll offsets and radiometer mounting offsets. The associated uncertainty of one standard deviation in light red shading accounts for temporal and spatial variations in satellite cloud retrievals.

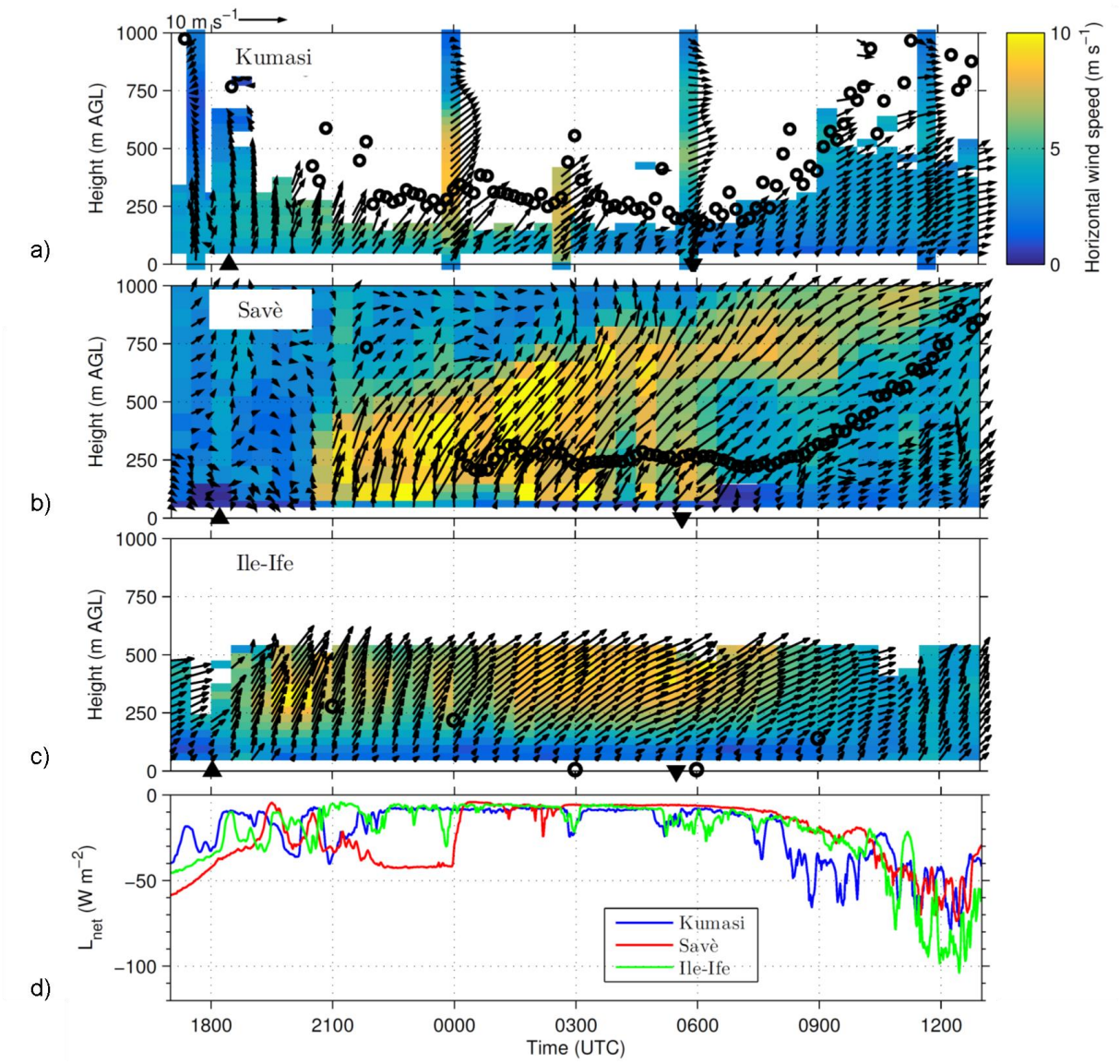

Figure 11: (a)–(c) Horizontal wind vectors (arrows), absolute value of wind speed (color-coded), and cloud base (circles) for the three ground sites Kumasi, Savè, and Ile-Ife, and (d) 1-min averaged net longwave radiation. The triangles in (a)–(c) indicate sunset and sunrise, respectively. In Kumasi the wind is derived from radiosondes and sodar, in Savè it is a composite of sodar and UHF wind profiler data, and in Ile-Ife it is based on sodar data. The cloud base height for Kumasi and Savè is derived from ceilometer data and is based on the algorithm of the manufacturers.

For Ile-Ife, the cloud base height is estimated from the relative humidity data measured with tethered radiosondes.

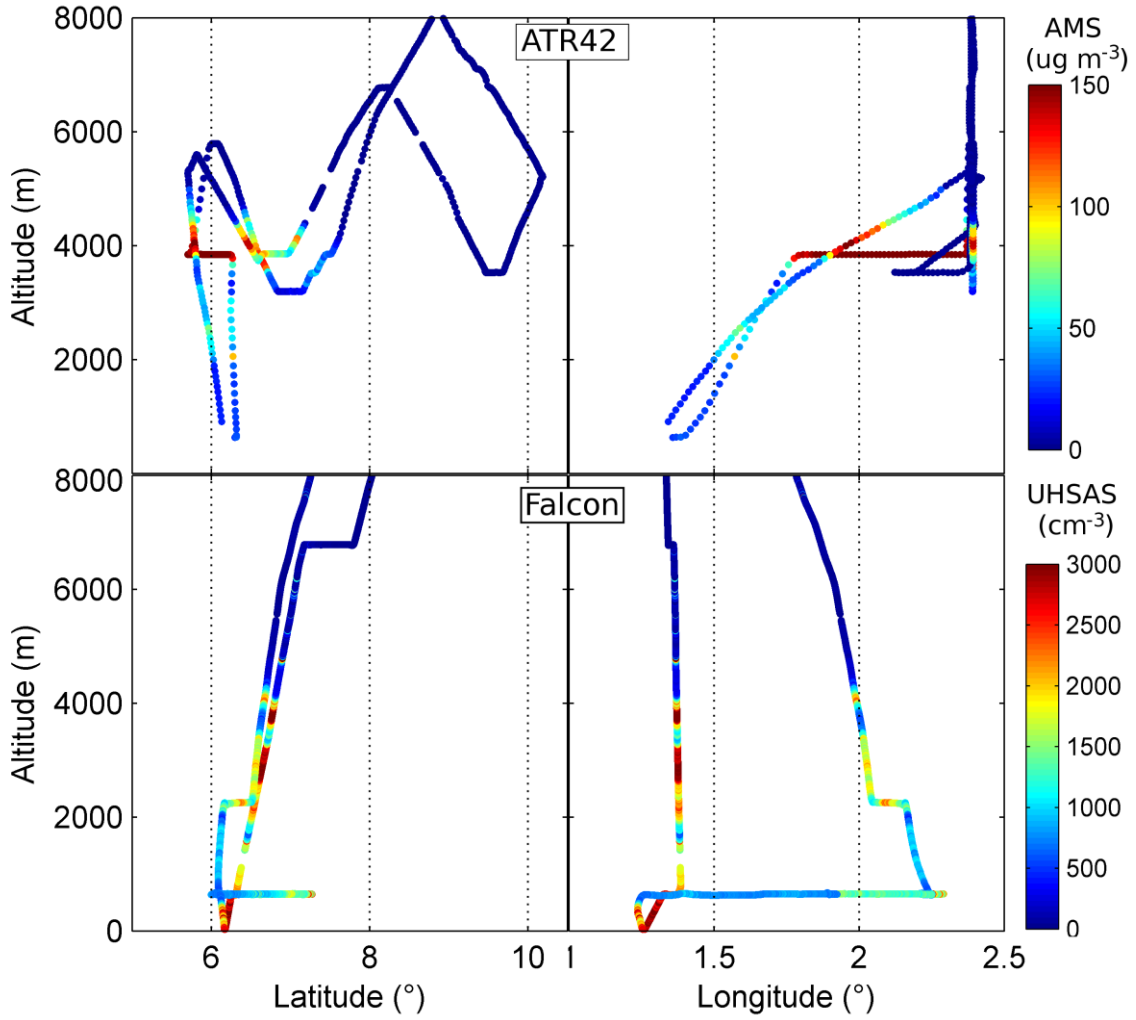

Figure 12. Left column: Latitude-altitude representation of the ATR 42 (top) and Falcon 20 (bottom) flight tracks on 13 July 2016. Right column: Longitude-altitude representation of the ATR 42 (top) and Falcon 20 (bottom) flight tracks. The ATR flight track is color-coded according to AMS-derived NR-PM1 concentrations and the Falcon flight track is color-coded according to UHSAS-derived aerosol concentrations. See text in Section 7e for details.

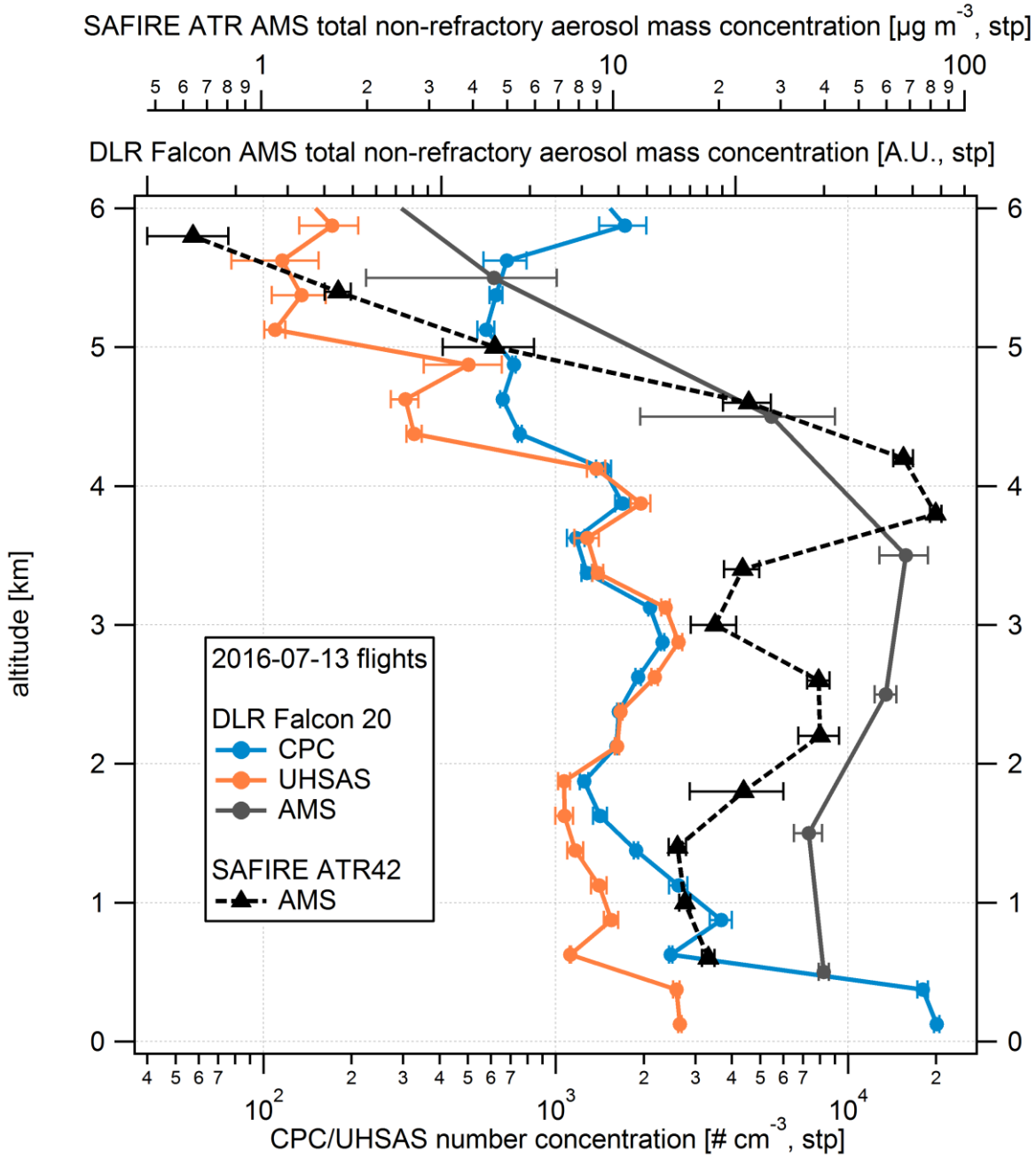

Figure 13: Profile of measurements from a Condensation Particle Counter (CPC, blue line), an Ultra-High Sensitivity Aerosol Spectrometer (UHSAS, orange line), and Compact Time-of-Flight Aerosol Mass Spectrometer (AMS) on board of the DLR Falcon aircraft (grey line) and ATR42 aircraft (black line) on 13 July 2016. The CPC and UHSAS measure aerosol concentration, with 10 nm cut-off for the former and 100 nm for the

latter. AMS data represented here are the sum of the submicron non-refractory species organics, sulphate, nitrate, ammonium, and chloride (NR-PM_1). Data points identified as clouds were removed from this analysis. All error bars in this figure represent the standard error of the mean of the data in the respective size bin, and do not include systematic errors.

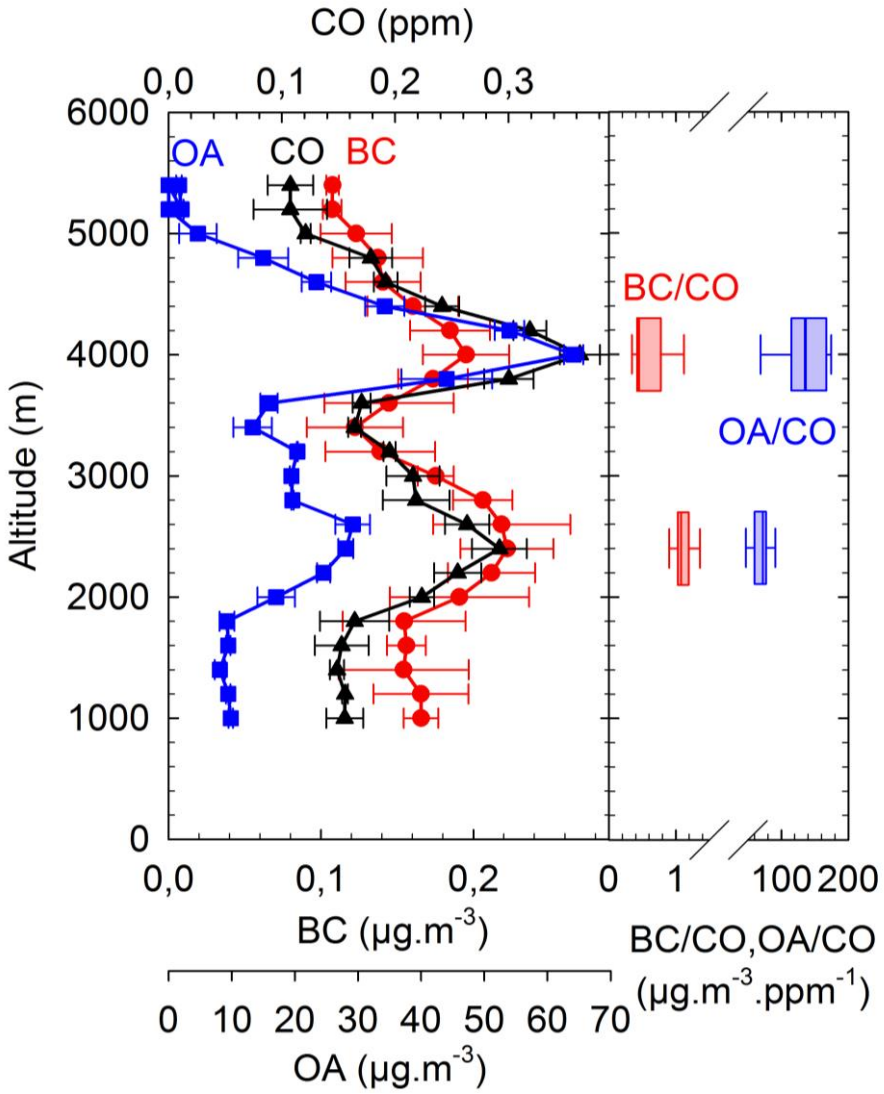

Figure 14. Vertical profile of black carbon (BC), organic aerosol (OA) and carbon monoxide (CO) (left panel) and the BC/CO and OA/CO ratio derived from these measurements (right panel). The points are mean concentration at each level and the bars through them are the standard errors.